Chapter 4

High-purity Refractory Metals for Thin Film Metallization of VLSI

Vadim Glebovsky

Additional information is available at the end of the chapter

http://dx.doi.org/10.5772/intechopen.69126

Abstract

It is shown that cast targets of highly pure refractory metals like W, Mo, Ti, Ta, Co, etc. and their compounds can be produced by means of a set of vacuum-metallurgical techniques—by vacuum high-frequency levitation, EB floating zone melting, EB melting, and electric arc vacuum melting as well as chemical purifying by ion exchange and halides. The cast refractory metal targets are extremely pure and chemically homogeneous. For magnetron sputtering and laser ablation, the cast silicide targets are also produced. The study reveals the possibilities and conditions of depositing the silicides and titanium-tungsten barrier layers by both the laser evaporation and magnetron sputtering. The physical and structural parameters as well as a trace impurity composition of sputtered metals and deposited thin films are studied by grazing-beam incidence X-ray diffraction, Auger electron spectroscopy, Rutherford backscattering of helium ions, mass spectrometry with inductively coupled plasma, etc.

Keywords: EB vacuum melting, target, magnetron sputtering, laser ablation, thin films, resistivity, refractory metals

1. Introduction

The application of thin films of pure Al and Al doped with Si (1 at.% Si) seems to be useful for the production of thin films for integrated circuits with dimensions of about 2 μm. A further reduction of dimensions to less than 1 μm and decreasing the *p-n* transition to 0.3 μm increase demands for parameters/operation conditions and necessitate a search for more reliable constructive and technological designs of the metallization including the contact units. Hence, ultra-purity is a term increasingly being applied to refractory metals [1–3]. Not only applications in the electronic industry but also their use as superconducting materials

or applications in the nuclear industry call for refractory metals and their alloys of utmost purity. The most intensive impact on ultra-purity of refractory metals is presently exerted by the electronic industry for VLSI applications [4–6]. In a word, VLSI means miniaturization. The goal of VLSI development is to find ways to pack as many tiny electronic components as possible into the smallest possible space. Often, smaller circuits also operate faster and, ultimately, drastically cut the overall cost of computation, opening up new possibilities for applications. Continued evolution of ever smaller devices has aroused a renewed interest in the development of new metallization processes for low resistivity gates, interconnections, and ohmic contacts. Al, W, and Mo are notable among the metals proposed for gate and interconnection metallization. The use of Al, however, requires all postgate processing of devices to be limited to very low temperatures, preferably below 500°C. The use of refractory metals, such as W and Mo, requires a complete passivation of these metals against oxidizing environments, a deposition by means that will not lead to unwanted traps in the gate oxide, and reliable etching of metals for pattern generation. Uncertainties associated with the stability of these metal films have led to a search for alternatives. As a rule, the different components deposited onto the Si substrate by different sputtering/evaporation methods must be ultrapure, especially with respect to trace contaminants listed in **Table 1** where the impurity compositions are represented for refractory metals studied in this chapter. The wide variety of applications of ultrahigh purity refractory metals as sputter targets in microelectronics is really impressive. A great number of companies compete to offer ultrapure refractory metal materials for sputter targets. Materials presently in the microelectronics use are W/Ti, Mo, $MoSi_2$, WSi_2, $TaSi_2$, $TiSi_2$, etc. As a rule, different components must be ultrapure, especially with respect to "mobile ions" (Li^+, Na^+, K^+, Ca^+, and Mg^+). With increasing miniaturization, an intrinsic radioactivity also exerts harmful effects; therefore, various components must be "free" of U and Th contamination. Nonmetals (O, N, H, and C) are detrimental too, as are impurities of Fe, Co, and Ni, for certain applications. However, information on analytical methods used for a chemical characterization of such materials as well as on metallurgical techniques used for a preparation of materials is extremely scarce or sometimes also misleading. It is known that a metal gate cannot withstand to the oxidizing annealing ambient and a source-drain formation by ion implantation is difficult because of the channeling of doping ions through the gate metal during ion implantation. In the process developed for MOS VLSI fabrication, W is used as the gate metal because a degradation of SiO_2 by annealing a $Me/SiO_2/Si$ structure at about 1000°C can be minimized. An oxidation of W is prevented by a moist hydrogen atmosphere during annealing. Si is also oxidized in the similar ambient. The most effective solution for VLSI is by applying barrier layers, such as Ti/W thin layers, nitrides, or silicides of refractory metals. The use of barrier layers requires a rational technique for their deposition as well as the materials of an optimal chemical composition. Even using Ti/W thin films as both barrier and conducting layers, the most suitable and advanced deposition technique is the magnetron sputtering, which is widely employed in commercial microelectronics. Thin films of Ti/W quasi-alloys as diffusion barriers for metal contacts on Si are used very intensively in the last decades. The W in this composition is supposed to serve as an interlayer diffusion barrier and the Ti as both a deoxidizer and a stopper of the grain boundary diffusion. The well-known channeling is stopped by forming a thin

Impurity	Mo	Ti	Ta	W	Nb	V	Zr	Hf	Co	Ni
C	0.1	30.0	30.0	4.0	40.0	20/0	50.0	50.0	10.0	0.5
O	0.5	400.0	5.0	1.0	5.0	200.0	100.0	10.0	20.0	–
H	0.2	–	2.0	0.1	1.0	–	–	–	1.0	–
N	0.05	5.0	5.0	5.0	5.0	5.0	5.0	5.0	7.0	–
Fe	0.5	10.0	0.5	1.0	0.5	8.0	300.0	3	50.0	0.1
Al	0.03	5.0	2.0	0.04	2.0	20.0	10.0	0.05	10.0	0.1
Cu	0.6	0.4	0.6	0.3	0.5	0.08	300.0	4	10.0	0.1
Ni	0.2	10.0	3.0	1.0	5.0	0.3	100.0	0.3	370.0	Matrix
Ti	0.2	Matrix	3.0	–	3.0	0.3	–	2.0	10.0	0.2
Si	0.3	0.6	1.0	0.04	5.0	2.0	1.0	0.5	15.0	1.0
S	0.3	0.2	0.2	0.1	5.0	2.0	–	–	10.0	–
P	1.0	1.0	1.0	0.5	1.0	0.5	–	–	5.0	–
Nb	2.0	2.0	30.0	1.0	Matrix	0.2	–	–	4.0	1.0
W	20.0	100.0	2.0	Matrix	30.0	0.3	–	0.3	10.0	1.0
Co	–	–	0.2	–	2.0	0.3	–	–	Matrix	0.1
Mo	Matrix	–	0.2	0.5	4.0	–	0.3	0.5	10.0	1.0
Ta	2.0	–	Matrix	1.0	50.0	30.0	–	–	5.0	1.0
Cr	–	0.3	0.3	–	0.5	0.3	5.0	1.0	10.0	0.1
Cd	1.0	0.7	0.3	0.1	0.3	0.2	–	–	0.1	0.2
Mg	–	0.5	0.2	0.1	1.0	2.0	10.0	0.1	10.0	0.1
K	0.4	8.0	1.0	0.02	1.0	1.0	1.0	–	1.0	0.3
Na	0.2	–	–	0.01	–	–	10.0	–	1.0	–
Li	–	–	–	–	–	–	10.0	–	1.0	–
Ca	1.0	1.0	0.3	1.0	1.0	1.0	1.0	1.0	10.0	0.1
Sb	1.0	0.7	0.3	1.0	0.3	0.5	1.0	–	1.0	–
Mn	0.2	0.3	0.3	0.03	0.3	0.1	1.0	0.1	10.0	0.1
Zr	0.3	0.3	0.3	–	0.3	0.3	Matrix	5.0	10.0	–
As	0.2	0.5	0.3	0.3	0.3	0.2	0.3	–	1.0	0.1
Pb	2.0	4.0	1.0	1.0	1.0	1.0	1.0	1.0	10.0	–
Zn	0.7	0.4	0.3	0.3	0.3	0.3	0.3	0.1	1.0	–
Sn	1.0	–	0.3	1.0	0.3	–	0.3	1.0	1.0	–
Bi	–	–	0.3	1.0	0.3	–	–	–	10.0	–

Impurity	Mo	Ti	Ta	W	Nb	V	Zr	Hf	Co	Ni
V	0.5	1.0	1.0	0.4	1.0	Matrix	1.0	1.0	10.0	–
U	0.005	0.006	–	0.005	–	–	–	–	0.005	0.05
Th	0.005	0.006	–	0.005	–	–	–	–	0.005	0.05

Table 1. Trace impurities in refractory metals participating in these studies.

layer of BPSG or WO_x on the W [4]. Because barrier layers in integrated circuits simultaneously serve as conducting layers, it is very important to have all possible information on their physical characteristics. However, electric characteristics of Ti/W contacts to Si, which have naturally to be dependent on the film stoichiometry, structure, and purity of Ti/W thin films, are not studied in a whole concentration range in the Ti/W system. The only experimental data available are results for Ti/W alloys with a mean content of 10–30 at.% W because these quasi-alloys are supposed to be optimal ones for microelectronics. Other problems aroused are connected with the preparation of sputter targets of a known chemical composition and required purity. A preparation of targets by the powder metallurgy (PM) techniques when compacted targets are manufactured using procedures such as powder mixing, hot pressing, hot rolling, and annealing is fraught with the contamination by a considerable amount of impurities, especially gas-forming ones. Thus, it can be said that the impurity content in targets prepared by PM techniques is predetermined by the preparation technique itself. As a result, there exists a possibility of a strong instability of the sputtering process due to an intensive gas release from the compacted powder target and even unpredictable fracture of sputtering components because of the explosive-like gas release at higher temperatures. It seems that a solution of this problem is in the combination of high-pressure techniques and in situ high-temperature annealing of PM compacted targets in a high vacuum [7]. Such a complex procedure allows one to produce PM compacted targets with a density which is nearly equal to the tabulated one of the material. An alternative to PM techniques is the use of cast targets produced from high-purity cast refractory metals without contaminating procedures like open-air hot pressing or hot rolling [8]. When it is necessary to prepare thin films of alloys, targets composed of cast metal blocks or co-sputtering of several cast metal targets can be used. It is known that TiW alloys cannot be produced by conventional melting procedures because of the great difference of their melting temperatures of both components. The sputtering or co-sputtering of cast metal targets seems to be the most promising ones owing to their flexibility and reliability, i.e., it is possible to obtain any necessary chemical composition of films due to the wide choice of compositions of "mosaic" targets, as well as deposition rates of each metal component during co-sputtering. One of the sections in the chapter will be discussing the experimental results of studies of the deposition of Ti/W thin films with different Ti/W ratios, made by magnetron sputtering of two cast metal targets, as well as of the dependence of the electrical resistivity on the Ti/W ratio. In other sections results of a deposition of thin films of other high-purity refractory elemental metals like Mo, W, Ti, and Co will be presented as well as the preparation of cast disilicide targets and deposition of thin films of disilicides for diffusion barriers of a high physical quality.

http://dx.doi.org/10.5772/intechopen.69126

2. Production of highly pure refractory targets and thin films

2.1. Purification of refractory metals

Naturally, in order to prepare highly pure sputter targets, the purest initial refractory metals are selected. For example, to produce the purest Ti sponge, the last versions of the Kroll process are included. Then a Ti sponge is elaborated with effective vacuum metallurgy techniques resulting highly pure metal Ti. In general, the basic way of a controlled purification of refractory metals from gas-forming interstitials and metal impurities is high-temperature vacuum melting or annealing. During this process the dissolved atoms of these impurities diffuse to the metal surface and desorb from it. According to modern representations [9, 10], the process of evolution of dissolved gas-forming atoms from the bulk of liquid metals to a vacuum consists of three successive stages: (*a*) a diffusion to the surface of the melt, (*b*) a transition through the interface to an adsorbed state, and (*c*) a surface recombination of adsorbed atoms with a formation and further desorption of diatomic molecules. Stage (*c*) in this chain is essentially nonlinear. Mechanisms of the O evolution depend on the metal nature and consist of the direct desorption of adsorbed O atoms in the atomic state and of the formation and further desorption of metal oxides of different stoichiometries. On the basis of principles of an evaporation deoxidation, the high-temperature behavior of O in refractory metals in vacuum can be roughly divided into three types. Ti, V, and Cr are characterized by a practically complete absence of the evaporation of O and metal oxides, because O in these metals is strongly bound with a metal matrix and has a very high thermal stability. The vapor pressure of the matrix metal (Ti, V, Cr) is much higher than other oxides of these metals. Mo and W are characterized by a high excess of the metal oxide vapor pressure above the metal vapor pressure; therefore dissolved and then chemosorbed O desorbs either independently or as metal oxides. Nb, Ta, Zr, and Hf behave intermediately. It seems that one has an opportunity for a preliminary estimate of the O behavior at the high-temperature vacuum treatment of both solid and liquid metals. A very different situation exists for C atoms which are strongly bound with metal and do not desorb independently. The basis of C evolution to vacuum is an interaction of O and C on the metal surface and further desorption in the form of gaseous CO. Naturally, it is very important to collect theoretical and experimental data on the behavior of such nonmetal impurities as O and C, because this information is a basis for the development of the commercial metallurgical technologies of the production of the high-purity refractory metals for microelectronics. A complex study has been fulfilled which allows one to establish the kinetic connection between the behavior of the mean concentrations of O and C. The dependence of this connection was studied on initial contents of gas-forming interstitials in liquid metals, as well as on the temperature, gaseous phase, and "diffusional transparency" of liquid metals. It has been shown that critical concentrations exist which are typical of each refractory metal. Below this critical concentration, O does not react with C, and the concentration of the latter during vacuum treatment remains constant. Experiments are also made, which demonstrated a high possibility of producing high-purity refractory metals. It has been shown that the "diffusional transparency," when diffusion does not influence chemical processes in liquid metals, can be realized in both vacuum levitation crucible-less melting and electron beam floating

zone melting because transport limitations can be removed by the constant renewal of the reaction surface. As for purifying refractory metals from metal impurities, it is important to emphasize that melting temperatures of refractory metals are high enough comparing with ones of many dissolved metal impurities in refractory matrixes. During high-temperature vacuum melting or annealing of refractory metals, dissolved atoms of gas-forming and metallic impurities diffuse to the metal surface and desorb from it. It means that there are optimal conditions for vacuum evaporation of metal impurities because their vapor pressure becomes very high at T_m of refractory metals. Optimal conditions of a vacuum refining have been identified and demonstrated a possibility of the production of Mo, W, Ti, Co, and other refractory metals having low contents of O and C (about 10^{-6} at.%) [11–16]. The opportunity has been demonstrated of the preparation of high-purity refractory metals, when contents of both C and O are at the determination level of the analytical techniques, such as deuteron activation, fast neutron activation, and mass spectrometry with inductively coupled plasma. The relationship between the purity of refractory metals and physical quality of deposited thin films was studied depending on the magnetron and laser sputtering conditions. This is not surprising since only gradually is it realized by scientific community dealing with these materials that the preparation of ultrapure refractory metals might be less difficult than a suitable and thorough trace chemical characterization. It is obvious that the analytic data at the ppb level are difficult to obtain and that interlaboratory comparisons exhibit a scatter of values, which is inversely proportional to the concentration level. This is a natural phenomenon symbolizing the state of the art of the analytical characterization of materials and should not be interpreted as an incompetency of analytical laboratories involved. **Figure 1** gives a rough estimate of the situation experienced by participants in many round robins analyses. However, a scatter of analytical round robin results, especially, on the ppb level of analysis is very hard—discrepancies between results of same samples but at different labs could achieve 100% and more. This is not too surprising that a scientific community has to understand gradually and to

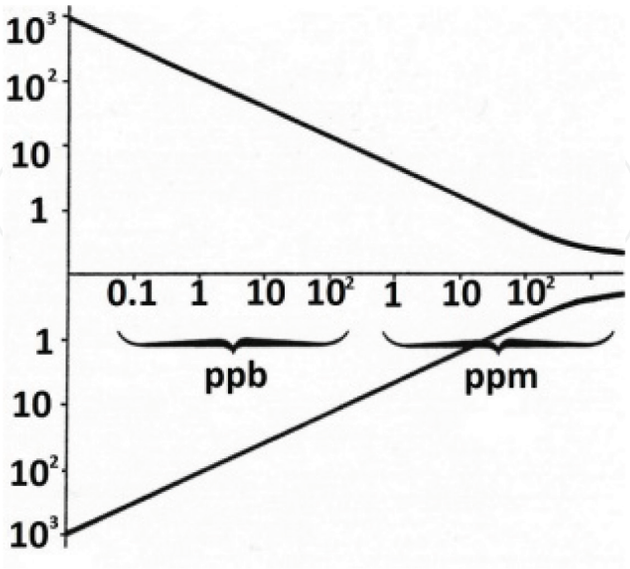

Figure 1. Scatter of round robin results at the trace and ultra-trace levels as a function of concentration levels of trace components.

realize when dealing with these metals that the preparation of ultrapure refractory metals might be less problematic than its elemental characterization [2, 3]. Analytic measurements at the ppm and ppb levels are difficult to obtain, and that interlaboratory comparisons exhibit a scatter of values, which is inversely proportional to a concentration level. This is a natural phenomenon symbolizing the state of the art of the analytical characterization of materials and should not be interpreted as an incompetency of analytical laboratories involved.

2.2. Technologies for production of refractory metals

Three main metallurgical procedures are developed to produce cast refractory metals of high purity for magnetron targets. Procedure #1 is the complex technology for producing elemental metal ingots/targets and bimetallic targets (e.g., Mo/Cu). It consisted of multiple electron beam (EB) vacuum melting of PM compacted blanks of refractory metals, hot pressing, hot rolling, electrochemical etching, electrochemical plating, high-pressure vacuum diffusion welding at high temperatures, machining, etc. Then the bimetallic Mo/Cu targets can be made of the Mo sheet and copper base joined together by vacuum diffusion welding. The upper high-purity Mo sheet of bimetallic Mo/Cu targets serves as a sputter material, whereas the Cu base serves as a heat-conducting material. Similar experiments are successfully done on other metal pairs such as Mo/Cu, W/Cu, Nb/Cu, NiV/Cu, etc. However, the most reliable results are obtained at the production of Mo/Cu. In spite of the lack of a reliable experience of using such targets in commercial sputter setups before, with this technology, hundreds of bimetallic targets are produced for several commercial microelectronics companies in Russia. Procedure #2 consists of multiple EB melting of PM compacted blanks in a vacuum of 1×10^{-6} Torr. Sometimes, the poly- and single-crystalline rods of EB floating zone melting can be used because they are much purer than PM sintered blanks. Two types of water-cooled copper molds, vertical and horizontal, are used for melting and solidification of round ingots of 80–150 mm in diameter and 1.300 mm length and flat ingots of sizes 35×100×1300 mm. Then ingots are carefully deformed and/or machined to get sputter targets. The rectangular and cylindrical molds are used to produce disks or plates of different sizes and diameters (80–210 mm). Procedure #3 is a duplex process, e.g., it consists of multiple EB vacuum melting and/or electric arc vacuum melting [16]. The liquid metal in the mold of the electric arc vacuum setup is intensively stirred by the electromagnetic field of the powerful electromagnetic solenoid. Thus, in this combination, EB vacuum melting is used mainly for a vacuum purification of liquid metals from gas-forming interstitials and metallic impurities, while electric arc vacuum melting is used mainly to produce ingots with a fine-grained macrostructure (this combination of techniques was used mainly for producing W or Mo).

2.3. Sputter of targets and deposition of thin films of refractory metals

Micro-metallurgy aspects imply a study of the magnetron sputtering and deposition of thin films and to study an influence of some parameters of the thin-film metallization on physical properties of deposited metal films. Refractory metal films are deposited on Si(100) wafers of 10–20 Ω cm with/without a thin film (about 0.3 μm) of SiO_2 at room temperature. The Si substrates are cleaned chemically prior to be loaded into the magnetron sputter apparatus. For

depositing thin films of metals, magnetron sputter apparatuses of two kinds are used: (*a*) the magnetron sputter system with the planetary arrangement of Si substrates for thin film depositing and (*b*) the conveyer system when Si substrates are deposited during traveling through different chambers of the apparatus. A special care is taken to exclude such contaminants as O, C, and alkaline metals from the apparatus environment. A vacuum at the sputter vessel is about 10^{-6} Torr prior to sputtering. Magnetron targets are cleaned preliminary for 40 min in vacuum. During sputtering, the vessel is filled with Ar of high purity to a pressure of about 10^{-3} Pa. The relative atomic impurity concentration of Ar is less than 3×10^{-6} %. Before sputtering, a heating of Si wafers to 250–300°C is carried out. It has been found that such a procedure is sufficient to produce a clean surface. The deposition rate is practically proportional to the sputtering power for high-purity refractory metals at a constant pressure in a sputtering vessel (**Figure 2**).

As-deposited films are annealed in vacuum. The sputter rate and layer thickness are controlled with the microprocessor and profilometer, respectively. The electrical resistivity of films is measured using a standard four-point probe. Generally speaking, film properties are affected not only by a deposition process as a whole but also by an initial quality of sputter targets. The specific resistivity of cast metal targets and thin films of highly pure refractory metals are shown in **Table 2**. It is well known that the specific resistivity of refractory metals is an integral characteristic of their purity. To study the influence of macro-metallurgical procedures,

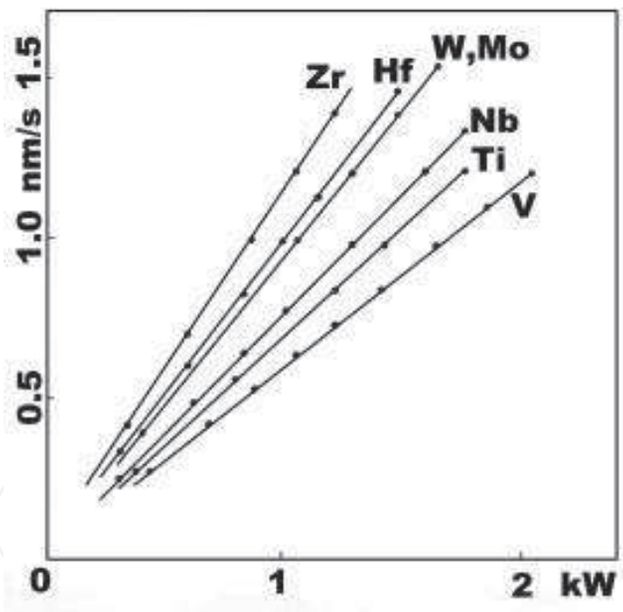

Figure 2. Dependence of a sputter rate for refractory metals on a sputter power at P_{Ar}=1 Pa.

Condition	Metal							
	Mo	**W**	**V**	**Nb**	**Ta**	**Ti**	**Zr**	**Hf**
Film	5.17	15.0	27.1	17.4	16.8	49.2	41.8	48.3
Target	5.2	5.5	25.0	–	12.7	41.7	–	–

Table 2. Specific resistivity of films and cast metal targets produced of highly pure refractory metals.

used for a production of targets, on the specific resistivity of thin refractory metal films, there are sputtered targets produced both by the standard PM procedure and EB vacuum melting. The content of gas-forming elements (C, O, N) in PM Mo targets is at least 100 times higher than in EBM Mo targets. It should be also mentioned that after prolong vacuum annealing of both targets and thin films, the content of gas-forming interstitials is still very high. The specific resistivity of Mo films of 0.15–1.0 μm thick deposited by sputtering the PM and EBM targets under the same sputtering conditions are 20–35 and 5.17 μΩ cm, respectively.

These results show that an initial purity of the target metal has a very strong influence on the specific resistivity of thin Mo films. After long sputtering, magnetron targets have an erosion path of about 10 mm depth and 20 mm width, and the further sputtering process is characterized by a little bit higher instability. The quantity of sputtered material is about 15–20% of the mass of the target depending on the target design and intensity of a sputtering process. This also shows that the design of targets and magnetrons should be optimal. An effect of a substrate heating on the specific resistivity is studied. When films are deposited on unheated substrates, their electric resistivity is increased by 50–150%, and the scatter of the specific resistivity is greater by 30–40%. This can be accounted for an influence of gas-forming impurities adsorbed on the surface of substrates. A confirmation of this fact is found in the lowering of the specific resistivity of Mo films deposited on unheated substrates with sublayers of Ti or V. These metals are sputtered from targets in the same sputtering vessel and probably react with gases adsorbed on a substrate surface. It is supposed that additional thin layers should not have a strong effect on resistivity measurements. To elucidate the influence of gas-forming impurities on the specific resistivity of refractory metal films, the sputtering power (or deposition rate) is varied and an air is introduced (1×10^{-5}, 4×10^{-3}, 1.3×10^{-4}, and 4×10^{-4} Pa m^3 s^{-1}) during sputtering. Experiments have confirmed that the specific resistivity of high-purity films of Mo, Ti, and Zr depends strongly on the deposition rate and on the presence of reactive gases in the deposition area (**Figure 3**). The ratio of the film resistivity ϱ_v to the target resistivity ϱ_m is a characteristic of the procedure as a whole: the higher the ratio, the less clean is the procedure. In other words, the specific resistivity of the films depends on the ratio of quantities of sputtered (deposited) atoms and interstitials dissolved in the metal films. The dependence of the specific resistivity on interstitials dissolved in the deposited film is studied (**Figure 4**). To analyze this dependence, the atomic concentration C_i of interstitials from reactive gases can be written as $C_i = (1 + \gamma_m S/\gamma_g S)^{-1}$, where γ_m and γ_g are specific rates of the metal deposition and condensation of molecules of *n*-atomic reactive gases in the refractory metal film, respectively, and S is a deposition area. The rate of dissolution of reactive gasses in the deposited metal film is much higher than the rate of a gas exchange in the deposition area of the magnetron sputtering setup, e.g., for the air leakage Q_i, we had $Q_i = \gamma_g S$. Here, it is assumed that the rate of dissolution of reactive gases in the film is constant. Because the quantity of metal atoms, $\gamma_m S$, which is sputtered in a unit time is nearly proportional to the sputtering power W, we had $\gamma_m S = kW$, where k is the coefficient of proportionality. This coefficient changes slowly with sputter parameters and is determined by dependence of the sputtering coefficient of refractory metals on the energy of sputtering ions and the geometry of the sputtering setup. Considering these equations, we can receive $C_i = (1 + kW/nQ_i)^{-1}$. This equation describes the dependence of interstitial content in the film on the ratio of the sputtering power to the reactive gas flow into the deposition area. The dependence allows us to present curves in **Figure 3** as the dependence of the specific resistivity on the atomic concentration of interstitials in films (**Figure 4**). The air leakage

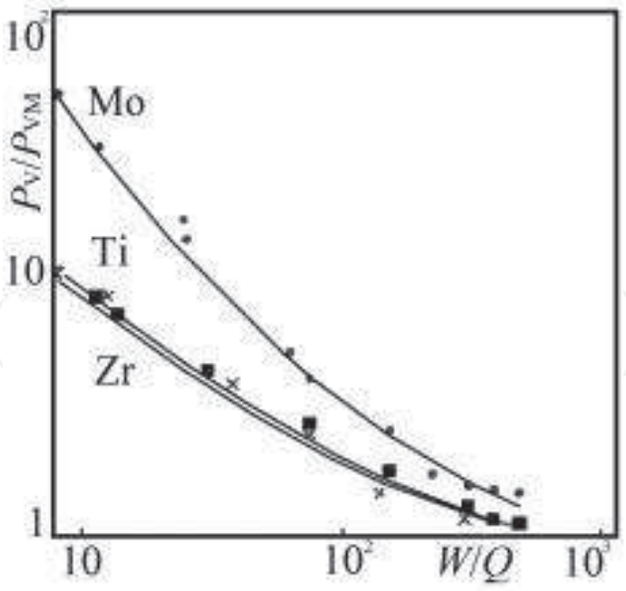

Figure 3. Dependence of film resistivity on sputtering power *W* and current leakage *Q*.

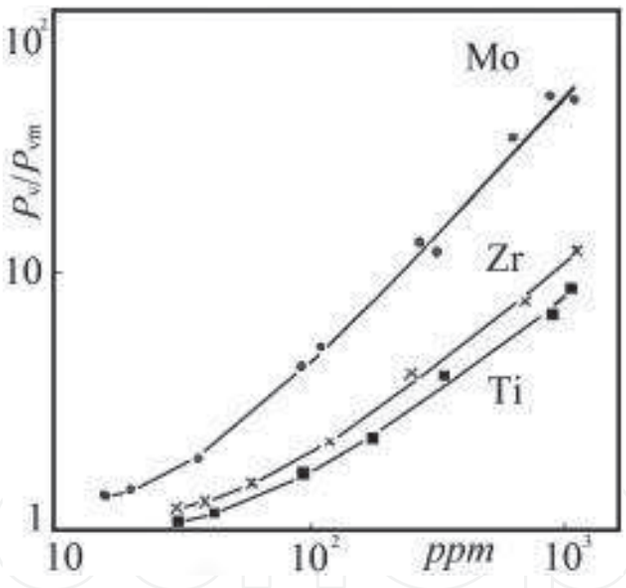

Figure 4. Resistivity ratio as function of interstitial content in the deposited films.

influence becomes very strong as the atomic concentration of interstitials in the film becomes higher than about 10^{-3} at.% (about 10 ppm).

2.4. Depositing molybdenum layers

2.4.1. Short background

Materials and technology of the deposition of thin metal films largely determine a level of performance and reliability of integrated circuits. Increasing the degree of integration and

performance of IC necessitates the search for materials and the development of a technology for the deposition of films in addition to or replacing the traditionally used Al (due to the appearance of high-temperature processes) and poly-Si having a high surface resistance. The renewed interest in the use in the IC of refractory metals, e.g., Mo [17, 18], nevertheless, is complicated by difficulties in obtaining films with properties of massive samples. Mo has a rather low specific resistivity and the closest to Si value of the coefficient of thermal expansion. It practically does not interact with SiO_2—the most widely used dielectric in the IC—and has a sufficiently high resistance to a mechanical damage. In addition, Mo forms ohmic contacts with Si with a comparatively low resistance (10^{-5} to 10^{-4} Ω cm^2). In [17], an interesting experiment is done by comparing a high-purity Mo target with a conventional one. It is shown that alkaline metals move easily in gate insulation films and deteriorate properties of MOS interface. The high-purity target which contains no more than 0.01–0.03 ppm Na and K and the conventional one with about 10 ppm of these metals are used in this experiment. The mobile ion quantity in the Mo gate MOS diodes which are produced with either the high-purity target or conventional one are compared before and after the annealing. Results show that no mobile ions are observed in the diode made with the high-purity target. The experiments conducted using W targets show similar results as well. By using several W targets which contained different amounts of Na, it is reported that there is a strong correlation between Na content and the amount of mobile ions in gate electrodes. In [7, 17], it is suggested that α-rays, directly radiated from electrode and interconnecting materials, are the worst factor in the operational reliability of the highly integrated VLSI. The amounts of α-rays radiated from Mo thin films formed by low or high U content targets are <1 and 700 ppb in the high pure targets and conventional targets, respectively; <1 and 280 ppb in the high pure Mo thin films and conventional Mo thin films, respectively; and <4.2 ×10^{-5} α cm^{-2} h^{-1} and 1.2 ×10^{-2} α cm^{-2} h^{-1} from the high pure and conventional Mo thin films, respectively. As can be seen from these results, there is a remarkable difference in amounts of α-rays which causes errors. Some decades ago, sputter targets contained several tens ppb and even ppm of U, while now in production scale, targets can often contain less than 1 ppb. EB evaporation makes it possible to obtain films with the specific resistivity ϱ_v = 15 μΩ cm only when the substrates are heated during the deposition to 400°C and higher. Cathode sputtering due to the high reactivity of Mo, low deposition rate (<0.5 nm s^{-1}), and difficulties in providing sufficiently small partial pressures of contaminating gas-forming impurities (O, N, H_2O, etc.) in the area of the discharge led to a relatively high level of the resistivity (higher than 30 μΩ cm). Magnetron sputtering systems that provide deposition rates at the level of 1–2 nm s^{-1} and above make the study of the feasibility of using this method of depositing refractory metal films for the fabrication of IC, in particular with MOS structures. It should be noted that such structures, *ceteris paribus*, are particularly sensitive to impurities such as alkali metals, which diffuse rapidly in the ionized state through dielectric SiO_2 films when voltage fields 10^5 V cm^{-1} are applied. This imposes additional conditions on the parameters of the target material and, of course, on film deposition conditions

2.4.2. Depositing molybdenum films

In our study [19] of Mo films, the procedure #1 is mainly used for purification and production of high-purity Mo targets. It is consisted of multiple EB melting of commercial PM bars/

rods at a melting rate of about 0.5 kg min^{-1} in a vacuum of 1×10^{-6} Torr. The power is 250 kW at an accelerating voltage of 25 kV and an emission current of 4 A. Two types of water-cooled copper crystallizers (molds) are used: cylindrical and rectangular. Analysis of the impurity content in Mo targets before sputtering is carried out by means of highly sensitive analytical methods: fast neutron activation, deuteron activation, mass spectrometry with inductively coupled ions, etc. The trace element composition of Mo targets is represented in **Table 1**. Mo films are deposited on Si(100) wafers (10–20 Ω cm) with/without a thin film (about 0.3 μm) of SiO_2 at room temperature. Substrates are cleaned chemically prior to load into a magnetron sputter apparatus. The sputtering chamber pressure is 10^{-6} Torr prior to sputtering; magnetron targets are trained for 40 min in vacuum. During sputtering, the chamber is filled with Ar of high purity to 10^{-3} Torr. Before sputtering, a heating of Si wafers at 250–300°C is carried out. It has been found that such a procedure is sufficient to produce a clean surface. The deposition rate is practically proportional to the sputtering power at a constant pressure in the sputtering chamber. The resistivity of samples of EB-melted Mo is 5.2–5.6 μΩ cm. The specific resistivity of Mo films 0.15–1.0 μm thick deposited from PM targets under same sputtering conditions is 20–35 μΩ cm. These experiments show that an initial purity of target has a very strong influence on the resistivity of thin Mo films. An effect of a substrate heating on the specific resistivity is also studied. An increased scatter of the resistivity is accounted for by the influence of gaseous impurities adsorbed on the substrate surface. To elucidate the influence of gaseous impurities in the specific resistivity of the Mo films, a sputtering power (a deposition rate) is varied, and an air leakage is introduced during sputtering. The experiments have confirmed that the specific resistivity of the films depends strongly on the deposition rate and reactive gases in the deposition area (**Figure 3**). The ratio of the film-specific resistivity (ϱ_v) to the target-specific resistivity (ϱ_{vm}) is a characteristic of the procedure quality: the higher the ratio, the less clean is the procedure. In other words, the specific resistivity of the film depends on the ratio of the quantities of the Mo sputtered (deposited) atoms and interstitials dissolved in the film (**Figure 4**). To obtain ingots free of pores and having a uniform distribution of impurities, a double run is sufficient with a melting rate 0.9–1.0 kg min^{-1}. As a starting material, the rods of commercial purity are used. The samples for the elemental analyses and metallographic studies are cut from the Mo ingot. A composition of trace impurities in the cast Mo under study can be seen in **Table 1**. The macrostructure of cast Mo ingots consists of grains with a length of 40–60 mm and an average diameter of 0.2–3 mm. As substrates for deposition, Si wafers of 76–100 mm in diameter are used, covered with a thermally grown SiO_2 of 0.05–0.3 μm thick. Mo films are deposited in a planar-parallel setup with the magnetron sputtering system. Relative to the target in a plane parallel to the target and situated at a fixed distance from it, substrates are linearly moved on which a metal film is deposited. The setup is continuously moving and equipped with gateways for loading and unloading substrates, providing the setup working without breaking a vacuum. In the setup used, the principle of a vacuum lock of the discharge area is used. As the working gas, a purified Ar is used, which is fed through a leak valve into a discharge area connected to a suction volume of diffusion slots for the passage of conveyor substrates. The pressure in the volume to feed airless Ar is less than 5×10^{-5} Pa and, in the process, less than 2.5×10^{-2} Pa; a discharge current is up to 15 A at a discharge voltage up to 600 V. The unit has an ability to preheat substrates by infrared lamps. Sputtering target composed of four elements is set out in a cooled holder. On

each element of the target, O-shaped sputter area (erosion) forms, whose length exceeds the width of the deposition area, thus ensuring the reproducibility of the thickness of the deposited layer on substrates with an accuracy of 2% (**Figure 5**). Ar flow during the deposition is 1×10^{-3} to 2×10^{-2} Pa m^2 s^{-1}. According to approximate estimates, a leakage of gas from the surrounding atmosphere in the discharge area is less than 1×10^{-5} Pa m^3 s^{-1}, which corresponds to the concentration of impurities introduced in the film less than 10^{-4} m.%. When depositing the films, it is revealed that the rate of Mo deposition, depending on the process conditions (Ar pressure, voltage, and discharge current) with accuracy of 10%, is a subject obtained by an analysis of the process. The length of the cathode dark space is determined experimentally by measuring a probe potential distribution in the discharge. In the field of real mode dispersion, it is not more than 0.1 cm, which corresponds to estimates by the formula of Child-Langmuir. Furthermore, the parameter $t = L/l \leq 0.2$ is defined, which greatly facilitates the integration of the equation. Dependence F for Mo is determined for voltages in the range of 300–500 V. The calculated dependence of the deposition rate in a normalized form concerning the conditions, under which there is no scattering of the sputtered Mo atoms on the Ar atoms, is shown in **Figure 6**. Experimental data are obtained by measuring a thickness of the layers deposited

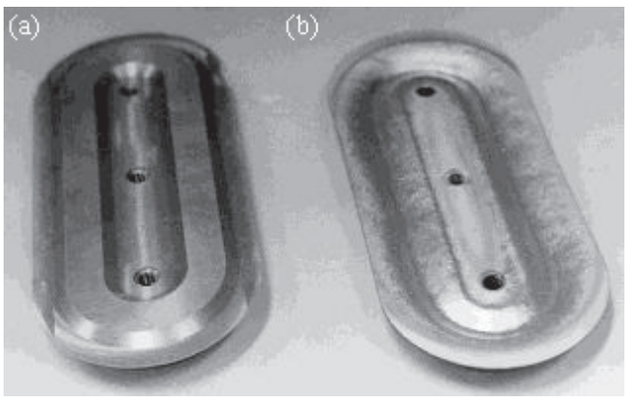

Figure 5. Two magnetron targets: new (a) and (b) after 200 cycles of sputtering.

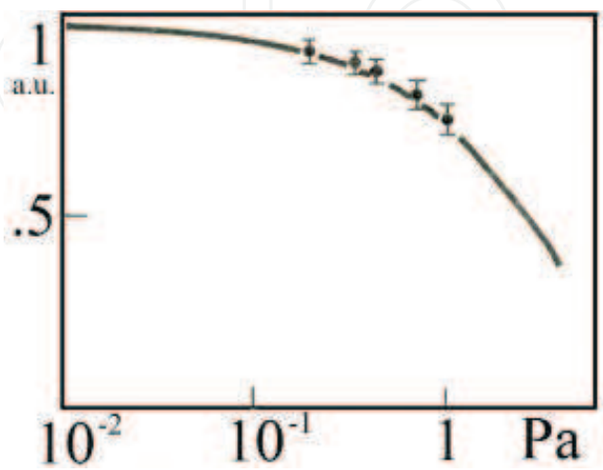

Figure 6. Dependence of deposition rate on Ar pressure: points, experimental data, and curve, calculated data.

under different conditions for specified periods of time. The thickness is measured with a precision micro-interferometer with accuracy of 300 Å. To correctly determine the deposition rate, the layers of 1 mm thickness are used.

To assess the quality of the deposited Mo films, the dependence of the resistivity is determined based on the Mo films on both the deposition conditions and the current-voltage characteristics of the MOS structure. The resistivity is calculated from the results of surface resistance measurements by four-point probe method and a Mo layer thickness with pre-coating a thin layer of Al (0.01 μm) to eliminate a phase distortion. Furthermore, after obtaining the deposition rate depending on the processing mode (the discharge voltage, current, and Ar pressure), the resistivity is determined from the measured surface resistance and the layer thickness calculated from the processing mode. It is found that the resistivity of Mo films in the thickness range of 0.15–1.0 μm with the deposition rate of higher than 1 nm s^{-1} changed a little, and its average value is 10 μΩ cm. Preheating the substrate reduces the resistivity to 8.5 μΩ cm, and it begins to depend on a layer thickness. Apparently, this is due to the influence of residual gases adsorbed on a wafer surface. It is interesting to note that when using PM Mo of a commercial purity (grade M−1) as an initial material for the target, a resistivity of the Mo films with a thickness of 0.5 μm cannot drop below 15–20 μΩ cm. To assess the specific applicability of the Mo films, test structures are fabricated on Si wafers with a resistivity of 7.5 Ω cm with orientation. The cross sections of a MOS test structure including the capacitor, element for determining the contact resistance of Mo-Si, and transistor are prepared. One of them (transistor) is shown in **Figure 7**. The fixed charge density in the oxide and fast surface states near Fermi level are determined on the high-frequency and quasi-static capacitance-voltage characteristics of the capacitor, which are, respectively, 5×10^{10} and 9×10^{10} cm^{-2}. Shifting the flat-band potential after a thermal treatment at 200°C and the field voltage $\pm2\times10^{6}$ V cm^{-1} does not exceed 50 mV for 5 min, which indicates the high stability of the obtained structures.

Measurements of the flat-band voltage on structures are made with a change in the dielectric thickness, depending on the allowed, to determine the difference between the work function of the metal semiconductor, $\Delta\phi_{ms}$, which prove to equal to −0.285±0.015 V. In the case of poly-Si gate, the work function difference is −0.9 V. It is known that a more positive value should significantly improve the current-voltage characteristics of the transistor with a short channel. In order to confirm the feasibility of this assumption, the transistors are

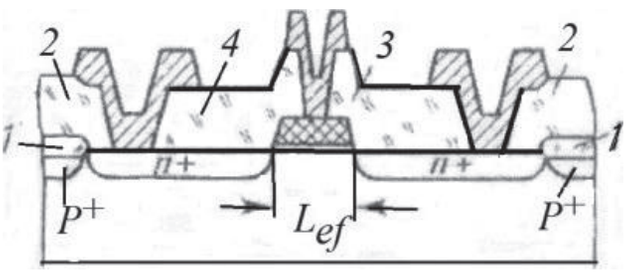

Figure 7. Test MOS structure (transistor); 1, SiO_2; 2, PS glass; 3, Mo; and 4, Mo+Al.

made with an effective channel of a length L_{ef} = 1.2 μm at the channel length L = 2.0 μm on the gate. To eliminate the effects of shortening the channel, ion implantation of the channel by B is made. Measurements show that the magnitudes of the threshold voltage U_t = 1.0 V at the voltage of "source-drain" U_{sd} = −2 V and the "source-substrate" U_{ss} = −2 V are reached on the transistors with gates made of poly-Si and Mo, respectively, at doses of 0.12 and 0.06 a.e. Comparing the current-voltage characteristics shown in **Figure 8** for the transistor of the same geometry, it is revealed that the design efficiency of a poly-Si gate is lower than the structure having a gate made of Mo. This is due to the fact that with increasing doping with B, there is a more severe degradation of mobility in the short channel as well as reducing the slope. Finally, along with the achievement of the resistivity of ~10 μΩ cm of Mo film, which is a very significant for use in IC as an element of their design, the ability has appeared to implement ohmic contacts with Si having a low resistance level, especially in the case of shallow (less than 0.5 μm) transitions. To clarify this possibility and evaluate the stability of the contact, the dependence of the contact resistance on heat treatment conditions is necessary for rapid annealing of surface states. The results (**Figure 9**) show that it remains at 2×10^{-6} Ω.cm. It is found that the specific resistivity of the contacts depends on the temperature of the heat treatment as well as the leakage current of n^+-p-transition on the level of ~10^{-8} A cm^{-2} is constant at various temperatures and duration of the heat treatment. Additional studies have confirmed that this is due to the formation of $MoSi_2$ at the boundary of Mo-Si. It should be noted that due to the fine-grained structure of Mo film (grain size of about 700 Å), a photoengraving provided receiving patterns of paths and the size of gaps between paths of about 3 μm and besides the restriction is limiting the possibility of obtaining the necessary quality patterns on a photoresist. The uniformity of the structure and the reproducibility of Mo film properties provided highly reproducible results in a large number of plates are confirmed as well. Thus, the studies show real possibilities and advantages of using highly pure Mo for obtaining VLSI.

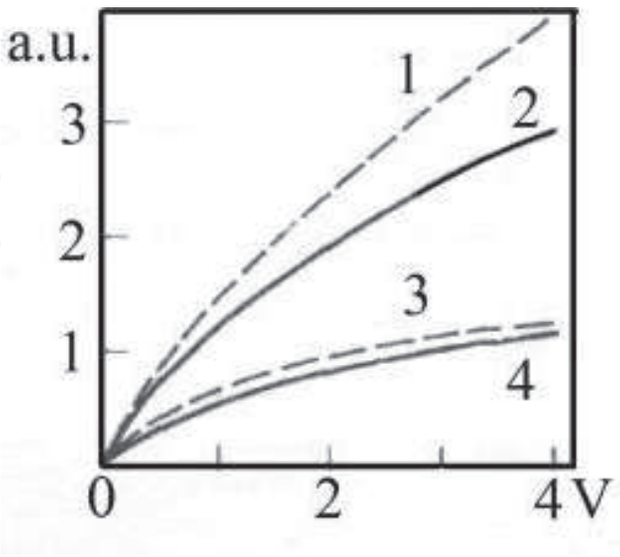

Figure 8. Current-voltage characteristics of transistors with the same geometry of gates produced of Mo (1, 3) and of poly-Si (2, 4); U_g: (1, 2) 4 V, (3, 4) 2 V; Δ_{SiO2}=400 Å; L_{ef}=1.2 μm.

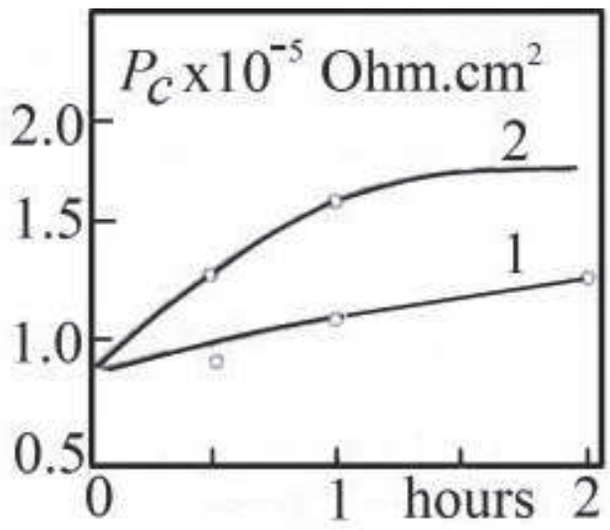

Figure 9. Dependence of contact resistivity on the temperature and duration of heat treatment which were necessary for rapid annealing of the surface states; temperature, (1) 450°C, (2) 475°C.

2.5. Depositing titanium-tungsten layers

2.5.1. Short background

Multilayer structures have become widely used in silicon VLSI technology to produce thin-film current-conducting systems. Normally, they contain contact layers, barrier layers, and base current-conducting layers. In some cases, barrier layers are simultaneously contact-to-Si layers. The reproducibility of the current-conducting system of silicon VLSI as a whole depends to the high extent on physical and chemical properties of diffusion barrier layers between the Si and Al. Naturally, properties of barrier layers connect with the purity of materials, the solubility of other chemical elements in the multilayer structure during thermal processing, interfaces between layers, and manufacturing techniques used. Chemical impurities dissolved in films should not cause any strong radiation damage during the process of film deposition. Current-conducting systems with Ti barrier layers are characterized by the formation of a $TiAl_3$ phase at annealing temperatures above 485°C, which leads to consumption of a barrier material. The solubility of Si in TiAl is several times higher than in Al. Therefore, if barrier layers are not sufficiently thick or contain defects, a degradation rate of the Si/Ti/Al or Si/PtSi/Ti/Al contacts may turn out to be unacceptably high. Films of TiW alloy exhibit a better combination of strength and plasticity than Ti, which considerably reduce a probability that vacancies and point puncture-type defects would be formed in films when residual mechanical stresses are high. It is interesting to study, simultaneously with general conditions of a formation of current-conducting systems, a variety of factors affecting properties of the layered current-conducting systems in VLSI structures. It is found that the content of Ti in TiW barrier layers can be varied in the range 12–43 at.% Ti. At the same time, Ti/W targets, sputtered or evaporated for the deposition of TiW barrier layers, contain no less than 30–40 at.% Ti. The correlation between the Ti content in sputter targets and in deposited thin layers is necessary to develop a controllable deposition process. However, such correlation is very difficult to find and achieve because it depends on

many different parameters, such as sputtering conditions, a chemical purity of metal components, a design of the sputter setup, and technologies used for the preparation of targets. To the best of our knowledge, no studies have been reported on using of Ti/W composite cast targets for the deposition of TiW barrier layers. In this chapter, scientific and technological results are presented on both the production of high-purity metals by the vacuum-melting technique and deposition of thin TiW layers by sputtering of composite targets [6, 7, 20–22]. When it is necessary to prepare thin films of alloys, targets composed of the cast metal blocks or co-sputtering of several cast metal targets can be used. As a rule all metallic components should be ultrapure, especially with respect to "mobile ions." With increasing miniaturization, the intrinsic radioactivity also exerts harmful effects; therefore, various components should be "free" of U and Th contamination. Gas-forming interstitials (O, N, H, C) are detrimental too. Because of strict requirements to the purity of refractory metals for microelectronics, all undesired impurities should be removed to less than the level of ppm level in order to be able to prepare extremely pure refractory metals or binary alloys based on such pure metals. Hence, considerable effort is necessary in the purification and doping processes. All process steps should be monitored by very sensitive and, generally, very expensive instrumental analytical methods down to a level even of 1 ppb with a special reference to the gas-forming elements which are extremely difficult to determine in metal materials.

2.5.2. Depositing titanium-tungsten layers by co-sputtering titanium and tungsten targets

The targets of 78 mm diameter and 6 mm thick are used for magnetron co-sputtering [20, 23]. They are machined from polycrystalline ingots of high-purity W and Ti (the metallurgical procedure #2). W and Ti disks for co-sputtering have the same sizes. The films are deposited by magnetron co-sputtering high-purity Ti and W disks which are fixed in water-cooled copper holders of the magnetron sputter setup. The Ar pressure is maintained automatically. Substrates of Si (10–20 Ω cm, 100 mm diameter) placed on a planar substrate holder are spun freely on their axis with 15 rotations per minute and moving in the circular zone which passes above the sputtering targets at a frequency of 30 rotations per minute. The distance between targets and substrates is 60 mm. A shield between them enables the preliminary training of targets and realization of necessary sputtering conditions. The substrates are cleaned chemically prior to load into the magnetron sputtering apparatus. Prior to the deposition, the apparatus is evacuated to 10^{-6} Torr; a leakage of gasses into the deposition area is no higher than 10^{-2} Pa s^{-1}. Before the deposition, the substrates are in situ heated to 250–300°C. A discharge power on each target is up to 2 kW; Ar pressure during a co-sputtering procedure is 10^{-3} Torr. Based on an assumption that the deposited layer density does not differ from that of a bulk metal, in order to obtain a necessary Ti/W ratio in the film, deposition rates of both metals are determined as a function of the discharge power at Ar pressure of 1 Pa. For that purpose metal films are deposited on thermally oxidized Si substrates at various discharge powers, the energy consumption during these processes being 400–600 kJ. This ensures the layer thickness of 0.5 μm and the possibility of their measurement with sufficient accuracy. Experiments show that the deposition rate of each metal depends linearly on the discharge power. **Figure 10** depicts dependences of mean and instant rates with respect to the thickness (γ_1 and γ_2, nm s^{-1}) and dependences of mean and instant deposition rates (γ_1 and γ_2, atoms

cm^2) on the discharge power. Six groups of film samples are prepared which differ from each other by quantities of monoatomic layers of Ti and W and by Ti/W ratios. Quantities of monoatomic layers of each metal in these six film specimens are shown in **Table 3**. Bearing in mind that the 1-mm-thick film area of 1 cm^2 contains 5.67×10^{15} Ti atoms and using experimental data of **Figure 11**, the sputtering discharge power for each target can be determined which is necessary to prepare homogeneous TiW films with definite but different Ti/W ratios. Because Ti layers alternated with W layers in the film structure, some lamination or layering of the film is possible. To escape this, vacuum annealing is done to make the structure of as-deposited films more homogeneous, which is confirmed by X-ray diffraction. The mean grain size of films with different chemical compositions measured by transmission electron microscopy is in the range 10–20 nm. The structure of samples 2 to 4 revealed by X-ray diffraction (**Table 3** and **Figure 11**) is found to be a solid solution of Ti in *bcc* α-W with a lattice parameter from 0.318 to 0.323 nm (by 0.5–2% larger than that for pure W films—*bcc* β-W has a lattice parameter a = 0.317 nm). The structure of pure Ti films is *hcp* α-Ti with a = 0.295 nm and c = 0.447 nm. Such a surprising result is supposed to be a consequence of intermixing of Ti and W atoms with high energies (1–3 eV), the mutual interdiffusion and an overlapping deposition zones during magnetron co-sputtering although the thickness of deposited layers is about 4 nm.

The specific resistivity of TiW thin films depending on the Ti/W ratio is studied using values of the surface resistivity and the film thickness (**Figure 11**). The resistivity of thin films of

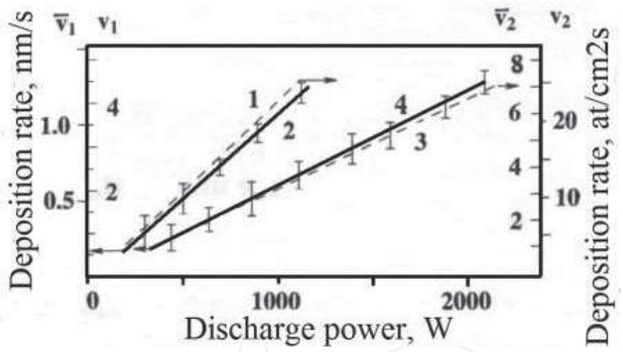

Figure 10. Mean and instant deposition rates as function of the film thickness.

Sample	Monoatomic layers	
	Ti	W
1	1.4	13.8
2	5.0	13.8
3	12.0	14.0
4	11.0	5.5
5	11.0	3.0
6	14.4	1.0

Table 3. Quantities of monoatomic layers of Ti and W in six film samples.

http://dx.doi.org/10.5772/intechopen.69126

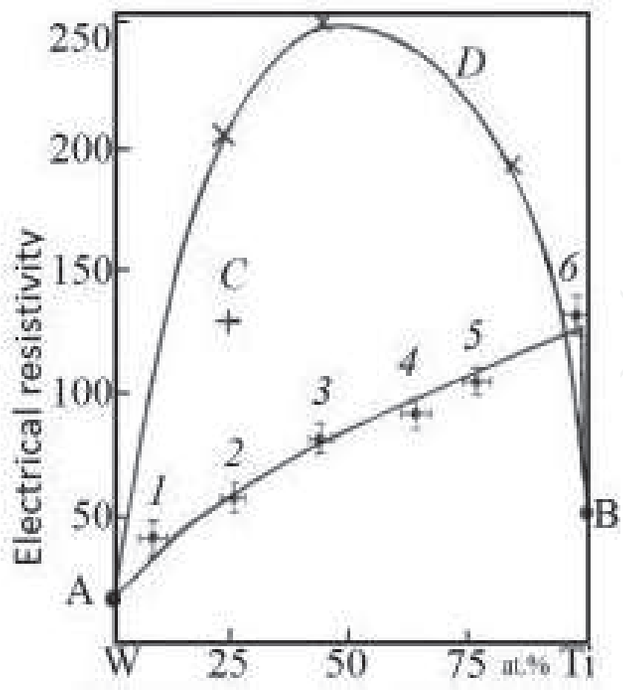

Figure 11. Dependence of resistivity of Ti/W films on Ti/W ratio. Points 1–6 [20], points of curve *D* [22]; point *C* for film deposited from PM target.

pure W and Ti is very near to the tabulated ones for bulk metals. They are shown in **Figure 11** as points *A* for W and *B* for Ti. The coincidence of the resistivity for films and bulk samples can be a characteristic of the quality of the co-sputtering procedure. The resistivity of films is increased gradually as the Ti/W ratio is changed from those for pure W to pure Ti. However, it is worth to mention that the resistivities of quasi-alloy films are always higher than those of pure metals. Such behavior of the resistivity of both pure metals and alloys is well known in physical metallurgy and can be explained by using physical models for a conduction of electrons in solids. From the physical point of view, the Ti/W quasi-alloy consists of two very different metals which have very different physical properties (densities, melting points, etc.) and phase structures (*hcp* and *bcc*). Thus, it is very difficult to make a reliable prediction of the resistivity curve behavior of these films depending on their chemical compositions. Experimental studies of physical characteristics of these quasi-alloys are of a great interest because of the necessity of getting the physical description of the composition, structure, etc. Another experimental fact which is also very surprising is the resistivity of TiW films with a small addition of W, as a dopant (1–4 at.%): the resistivity of a doped Ti became higher than the specific resistivity of pure Ti films. Contrary to this fact, the difference between the resistivities of both pure W films and TiW films with a small addition of Ti as a doping element increases gradually. At the moment there is no a reliable explanation of this interesting fact. Comparing our data with those of Babcock and Tu [22], values of the specific resistivity of thin films deposited by co-sputtering of high-purity cast metal targets are much lower than those of [22]. The discrepancies between the results of these two studies are evidently the consequence of using cast metal targets of higher purity in our study [20] as well as a more advanced deposition procedure. Another result, which is also of some interest, is the

difference between the resistivity of films deposited from two kinds of sputtering targets: cast metal targets and PM Ti/W powder targets. By sputtering of targets compacted from high-purity Ti and W powders with W content of 25 at.% by PM techniques, vacuum-annealed films have the specific resistivity of 130 μΩ cm (Point *C*, **Figure 11**). Auger spectrometry of films which are obtained by magnetron sputtering of PM targets shows the presence of high contents of C and O, 5 and 4 at.%, respectively. In layers obtained by co-sputtering of cast metal targets, C and O contents are lower than 1 at.%.

2.5.3. Composite titanium-tungsten targets for deposing barrier layers

Metallurgical technologies to produce of Ti/W targets are selected according to procedure #1 [24]. Multiple EB vacuum melting of compacted Ti blanks is used, as well as cold/warm/hot rolling, cutting, drilling, pressing, etching, polishing, etc. By this procedure, cast Ti polycrystalline disks of 190 mm in diameter and 23 mm thick are prepared. For this purpose, Ti rods produced by iodide process are preliminary carefully purified by EB floating zone vacuum melting and then remelted by EB vacuum melting in specially designed water-cooled copper molds. At the same time, highly pure W single-crystalline rods of 11 mm in diameter and 350 mm length are purified by EB floating zone vacuum melting. Composite cast Ti/W targets consisted of Ti disks with W cylindrical attachments, arranged in such way that the ratio between the areas of Ti and W sections on sputtered targets surface corresponds to the necessary Ti/W ratio in deposited films (**Figure 12**). TiW films are deposited by sputtering composite Ti/W, contained 40 at% of Ti, in a sputter deposition system with d.c. power of 2.4–3.2 kW. Leakage currents are measured at a reverse bias voltage of 15 V. The current density during sputtering is about 0.1 A cm^{-2}. The sputtering yields of Ti and W are the same; however, they are chosen to obtain the necessary Ti/W ratio during the whole sputtering procedure. The deposition rate is about 1.8 nm s^{-1}. Films are deposited on *n*-Si(111) substrates (100 mm in diameter) preheated in vacuum by IR lamps to 250°C with accuracy of 5°C. Test Schottky diodes with both *n*-Si/PtSi/TiW/Al and *n*-Si/PtSi/Mo/Al structures are formed by standard techniques. These techniques consist of (*a*) deposition of thin Pt layers by cathode sputtering on Si substrates through contact windows of 10 μm × 15 μm which are formed in a surface thermal SiO_2 layer, (*b*) annealing of the PtSi structure and removal of the unreacted Pt, (*c*) magnetron sputtering of TiW or Mo, and (*d*) deposition of the upper Al layer by d.c. magnetron sputtering of A1-1 at.% Si target. Photolithography and etching are used to obtain contact windows. The structures are annealed in a nitrogen atmosphere at 450°C for different times, but not more than 3 h. The temperature of Si substrates is measured indirectly by a calibration

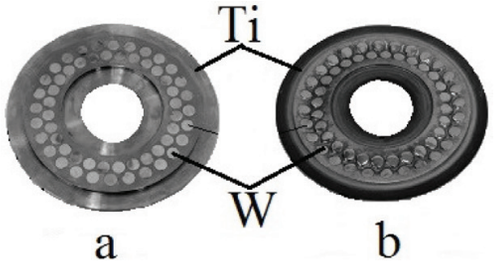

Figure 12. Composite sputter Ti/W targets (left, new; right, after 150 cycles).

or thermal painting. During measurements of mechanical stresses, the heating of all samples is carried out in the same way. The thickness of TiW films is 0.18 μm with accuracy of 0.02 μm. The sheet resistance is 3.5–4.5 Ω/□; the specific resistivity of TiW films is 65–72 μΩ cm. The samples are analyzed by four-point probe sheet resistance measurements, scanning electron microscopy, Auger electron spectroscopy, X-ray diffraction, X-ray electron probe spectroscopy, and laser ellipsometry, enabling an evaluation of residual mechanical stresses in films to be made with error of 2%. The leakage currents and Schottky barrier heights are registered with accuracy of 0.5 and 0.1% over the measurement range, respectively. XRD data show that TiW films are solid solutions of Ti in a W matrix with increased W lattice parameters. A relative increase in the W lattice parameter depends on a quality of surface conditions (polished or unpolished) of Si substrates on which films are deposited (**Figure 13**). The relative increase in the W lattice parameter for a polished surface was $\delta d/d0 = 7\times10^{-3}$, while for an unpolished surface, it is $\delta d/d0 = 2\times10^{-3}$. Here $d0$ is the lattice parameter of W (from ASTM tables). This difference is mainly due to the action of residual mechanical stresses in films. Measurements of a curvature of Si substrates with WTi films show that bending radii were $R_{1b} = 47.0$ m and $R_{2b} = 64.5$ m for polished Si substrates with/without a thermal SiO_2 sublayer on the Si surface. Bending radii are $R_{1b}' = 69.0$ m and $R_{2b}' = 103.0$ m for unpolished Si substrates with/without thermal SiO_2 sublayer. Mechanical stresses of specimens with/without SiO_2 sublayer correlate with a microstructure of TiW films. Mean grain sizes of TiW films are 35 and 45 nm for samples with/without SiO_2 sublayer, respectively. **Figure 13** shows microstructures of surfaces of TiW films on the polished Si substrate with (*b*) and without (*a*) the thermal SiO_2 sublayer.

The bending displacement is reciprocally related to the bending radius of the substrates, and so it can be supposed that mechanical stresses in films deposited on unpolished substrates are lower than those in films deposited on polished substrates. This correlates with values of relative deviations of the lattice parameter for unpolished and polished substrates ($\delta d/d0 = 2\times10^{-3}$ and 7×10^{-3}, respectively). The absolute value of the bending displacement can be used to estimate resulting mechanical stresses in the sample. Values of bending radii for samples without SiO_2 sublayers are higher than for samples with SiO_2 sublayers on both unpolished and polished Si substrates. These results confirm the observations of the dependence of mechanical stresses in thin layers on properties of the material and its crystallographic microstructure. It can also be supposed that SiO_2 sublayers change conditions of nucleation and growth of TiW films. As a result, there is a more spontaneous formation of nuclei, faster unity, and higher resulting stresses localized on grain boundaries. The influence of sublayers on the layer

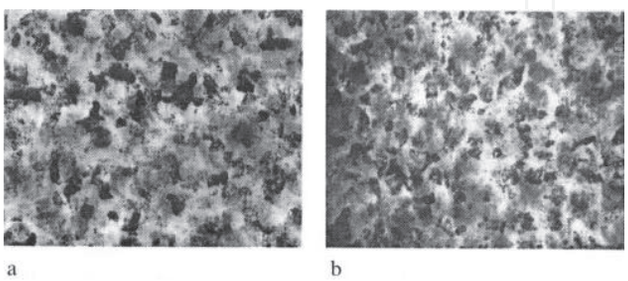

Figure 13. Scanning electron micrographs of the surface morphology of samples with structure Si/TiW (polished Si substrate) (a) and Si/SiO_2/TiW (b) (×100,000).

microstructure is confirmed by experiments in which Al layers are deposited onto both Si substrates and Si substrates with TiW film. The influence of a sublayer material on the film microstructure is studied on Al layers, prepared by magnetron sputtering of Al targets doped with Si (1 at.%), onto Si substrates with/without TiW sublayer. **Figure 14** shows a microrelief of Al films deposited on Si substrates without (*a*) and with (*b*) the TiW sublayer. The microstructure of the Al film in the Si/Al structure is rather smooth, and the Al film consists of coarse grains with a mean grain size of 1.1–1.3 μm. The mean grain size of Al films in the Si/TiW/Al structure is lower (about 0.3 μm) than in the Si/Al structure. TiW films, deposited by magnetron sputtering of composite cast TiW targets, contained approximately 40 at.% Ti, with a remainder W. Because TiW films serve simultaneously as current-conducting and barrier layers, sputtering targets should have a relatively high W content, together with the necessary Ti/W ratio for both optimal barrier properties and lower electric resistivity of TiW films. For effective barrier properties, it is preferable to have the Ti content in a range 30–40 at.% Ti in TiW thin films.

As shown earlier, the specific resistivity of TiW films increases with decreasing the W content to 98 at.%: the specific resistivity for this alloy is approximately 2.5 times higher than that for pure Ti films. The difference in the specific resistivity in the range of 30–40 at.% Ti is not large: 60–70 μΩ cm. To meet the requirements of the composite target design, the Ti content of 40 at.% is chosen. An excellent correlation between Ti/W ratios of targets and of films during the whole lifetime of sputtering targets is found, despite the fact that sizes of the erosion area changed significantly. The contents of the Ti and W components in the films vary slightly after 130–150 sputtering cycles. The relative deviation of the Ti content from the standard one during the target lifetime does not exceed 2 rel.%. Our AES studies of TiW films have revealed low concentrations of interstitials, such as O, C, and P. Auger profiling data of unannealed specimens are shown in **Figure 15(a)**. A typical result for these films is a sharp decrease of O and C contents during the etching process and a deepening of the analyzing zone. The behavior of O and C is very similar, and their curves partially overlap. Mechanical properties and microstructure of TiW layers also depend on the content of gas-forming interstitials, e.g., O, C, and H, even when they are present in very small quantities. It is unclear how strong the influence of a low content of interstitials is on physical properties

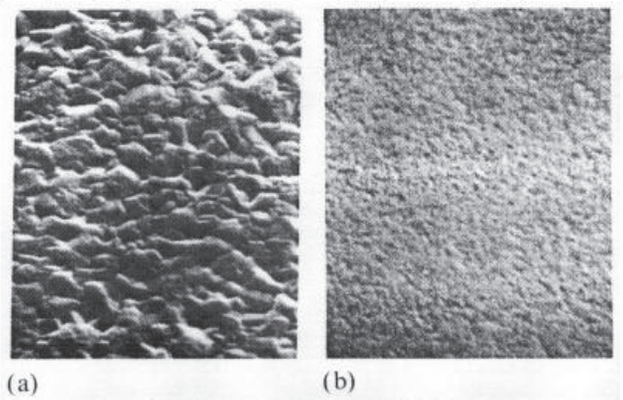

Figure 14. Scanning micrographs of the structure morphology of samples with structures Si/Al (a) and Si/TiW/Al (b) ×100,000.

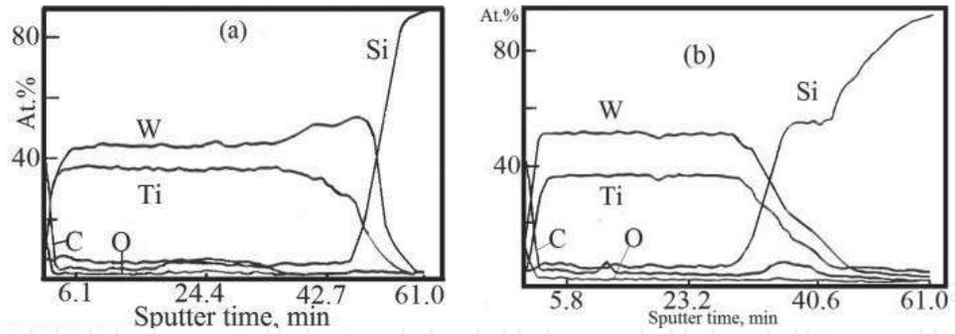

Figure 15. Auger electron spectra of samples with structure Si/TiW: (a) Auger electron spectra of samples with structure Si/TiW before (a) and after (b) isothermal annealing at 510°C for 1 h.

of thin films, although it is well known that interstitials, even at low concentrations, form very stable fine chemical compounds like refractory metal carbides, oxides, nitrides, etc., which precipitate on boundaries in thin metal films and can serve as boundary diffusion stoppers. On the other hand, the lack of discontinuities on the curve for C at an etching time of 50 min, e.g., near the Si/TiW interface, confirms both the effectiveness of the preparation of Si substrate surfaces before deposition and the sufficient cleanliness of sputter and deposition processes, at least at initial stages. A slight monotonic decrease in the Ti content near the Si/TiW interface is probably connected with an increase in the W content near the interface. It may also be a result of the nucleation of TiW films, which is preferable for W atoms because TiW films are based on the W lattice. It may also be associated with the fact that the coefficient of a W self-diffusion is much higher than the coefficient of a Ti self-diffusion (1.88×10^{-8} and 6.4×10^{-8} cm^2 s^{-1}, respectively). This may promote an easier motion of W atoms on a nucleation front during the film growth, as well as more frequent collisions of W atoms with a nuclei, and hence a higher probability of their accumulation on the nuclei. As can be seen from **Figure 15(a)**, W and Ti are homogeneously distributed throughout the film depth, which is probably a consequence of their interdiffusion. Near Si/TiW interface, there is a rather extended silicide layer, as can be seen from a monotonic change in the Si curve. Some localization of C near Si/TiW interface can be related to the differences in a C limited solubility and a C diffusion coefficient between the initial TiW film and the transition silicide layer detected near the SiO_2/TiW interface. The considerable O content in TiW layer is dependent on the fast O diffusion, compared with the self-diffusion of components of TiW alloy, and the high O solubility in W and Ti as well as in their silicides. If no Ti_xW_y is present in a solid solution, it is possible that Ti may display deoxidizing abilities and react with the Si recovered from SiO_2. In this case, a nonstoichiometric Ti silicide phase should be formed, because the formation of the stoichiometric $TiSi_2$ phase is not observed at such low temperatures. This supposition is in agreement with a monotonic change in the Si curve which correlates with a similar O curve. A temperature effect results in the depth redistribution of chemical components and impurities of TiW film. **Figure 15(b)** shows the Auger profiles for the depth distribution of elements in TiW films, isothermally annealed at 510°C in vacuum for 1 h. The W and Ti are homogeneously distributed throughout the film depth which is probably a consequence of the interdiffusion. At the Si/TiW interface, there is a rather extended silicide layer as can be seen from a monotonic change of the curve for Si. An increase in the C content

at Si/TiW interface can be related to differences in the C limited solubility and the C diffusion coefficient between initial TiW film and the transition silicide layer.

TiW films with a junction depth of 0.18 μm are tested as barrier layers on diodes with a square shape (10 μm × 15 μm). Schottky barrier heights on *n*-Si are determined from the current *vs*. applied voltage measurements. TiW layers form a relatively low Schottky barrier contacts to *n*-type Si (no higher than 0.5–0.6 eV). Curves 1 and 2 in **Figure 16** show the dependence of leakage currents on the testing time at 450°C in nitrogen. For comparison, barrier layers of Mo are also tested (**Figure 16**, curve 3). The measurements of the direct breakdown potential (U_0) for structures with TiW layers have revealed their high thermal stability after testing at 450°C for 3 h in nitrogen. A similar testing of structures with Mo layers shows that they are of a lower stability than structures with TiW layers (**Figure 16**, curve 3). Our experimental data on the testing of TiW barrier layers are associated with both the microstructure and morphology of Si-Me interface in contact with barrier layers of TiW or Mo. It is worth noting that leakage currents can be lowered by optimizing the technological procedures, for example, by a choice of a sputtering power (**Figure 17**). A higher quality of contacts with TiW barrier

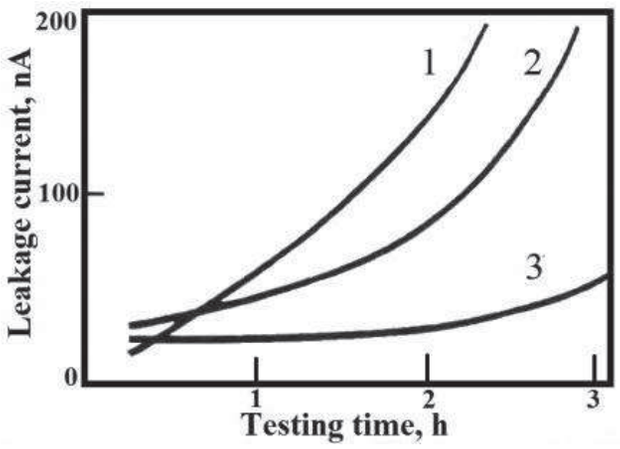

Figure 16. Leakage currents of samples with Schottky barrier diode structures *n*-Si/PtSi/TiW/AI and *n*-Si/PtSi/Mo/Al tested at 450°C in nitrogen: (1, 2) TiW films deposited at sputter deposition powers of 2.4 and 3.2 kW, respectively; (3) Mo film.

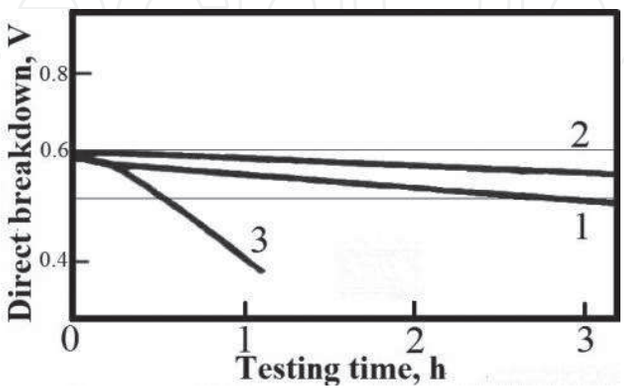

Figure 17. Direct breakdown voltages of samples with Schottky barrier diode structures at a current of 300 pA: (1, 2) structure *n*-Si/PtSi/TiW/Al (sputter deposition powers of 2.4 and 3.2 kW, respectively); (3) structure *n*-Si/PtSi/Mo/Al.

layers, obtained at an increased sputtering power, is partly due to a higher dispersion of the microstructure. Schottky diodes with TiW films exhibit a higher level of leakage currents than diodes with Mo films, although in both cases leakage currents are not an obstacle to the commercial use of these highly pure refractory metals as Schottky diode barrier layers. On the other hand, a great advantage of Schottky diodes with the Si/PtSi/TiW/Al structure is a rather high thermal stability of a direct breakdown potential U_0). A maximum deviation of U_0 from the mean value for structures with TiW layers is no higher than 0.1 V during thermal testing at 450°C for 3 h in nitrogen (**Figure 17**, curves 1 and 2). At the same time, the maximum deviation of U_0 from the mean value for structures with Mo layers is twice as high after a thermal testing at 450°C for 1 h in nitrogen (**Figure 17**, curve 3).

2.6. Depositing films of refractory metal silicides for barrier layers

2.6.1. Depositing films of refractory metal disilicides

Refractory metal silicides have a large potential as materials for the low-resistance contacts, gate electrodes, and interconnections in microelectronic devices [24, 25]. One of the well-known techniques for preparation of silicide layers involves a laser co-evaporation and magnetron co-sputtering of pure metal films onto a surface of a Si substrate with a subsequent high-temperature annealing. Another is magnetron sputtering or laser evaporation of silicide targets produced by PM or vacuum melting/casting. Casting of silicide ingots of commercial sizes is a well-known metallurgical problem because all refractory metal silicides are very brittle and hard in mechanical working. The optimal method is production of composite cast refractory metal silicide targets (cast silicide pieces are attached to copper bases by ultrasonic soldering). Vacuum melting and casting refractory metal silicides for targets solve the two main problems of thin-film deposition, i.e., desired chemical composition and high purity of thin films. The most problematic is a production of cast WSi_2 targets for the laser ablation or magnetron sputter because it is necessary to use two vacuum techniques—vacuum HF levitation and EB float zone melting. Rectangular cast WSi_2 targets used in this study [26] for laser ablation have a volume of 1.5 cm^3 and are chemically homogeneous. For magnetron sputtering composite, cast silicide targets of 152 mm in diameter are produced. Our study has revealed possibilities of depositing WSi_2 films by both the laser evaporation and magnetron sputtering. Other refractory metal silicides are produced in a similar way. Three experimental series are conducted to obtain silicide films: (1) laser evaporation of cast silicide targets, (2) magnetron sputtering cast silicide targets, and (3) magnetron co-sputtering of metal and Si targets. Initial materials for silicide sintering are 5N-purity Si and high-purity refractory metals (**Table 1**). Homogeneous mixtures of high-purity Si and refractory metal are prepared and isostatically pressed. Then mixture samples are sintered in a vacuum at 1100°C for 3 h. PM sintered samples are melted by vacuum HF levitation and cast in copper molds. The levitation melting consists of suspending a solid sample in HF electromagnetic field and melting it by the induced electrical currents. The resulting 25 g liquid drops have a form of the sphere. To solidify a liquid drop, it is enough to switch off an electric power. During laser ablation, the 10×15×5 mm^3 cast targets are evaporated with a solid-state Nd-laser of 1.06 μm wavelength, 0.8 J pulse energy, and 10–20 Hz pulse frequency [26]. The laser beam spot is 2–3 mm in diameter.

The substrates are Si(100), Si(111), MgO, ZrO_2, and Al_2O_3. The substrate temperature is varied within the range of 100–750°C. The deposition time is 5–20 min and a film thickness 15–200 nm. Magnetron sputtering involves the sputter cleaning of cast targets and sputtering films in Ar. Magnetron co-sputtering is as well used to produce many other refractory metal silicides (Ti-Si, Zr-Si, Hf-Si, V-Si, Nb-Si, Ta-Si, Mo-Si, WSi_2, $CoSi_2$, etc.). The sputtering system is first evacuated down to a vacuum of 2×10^{-6} Torr prior to the deposition of thin silicide films. Si wafers are cleaned chemically prior to load into a magnetron sputter apparatus. A special care is taken to exclude such contaminants as O, C, and alkaline metals from an apparatus environment. The sputtering procedure involves sputter cleaning cast silicide targets in Ar for 5–10 min, while the shutter is closed and sputters depositing silicide films in Ar. The relative atomic impurity content in Ar is less than 3×10^{-6}. The resistivity of thin disilicide films as well as cast disilicide targets is shown in **Table 4**.

2.6.2. Depositing films of WSi_2

During magnetron sputtering, the WSi_2 films are deposited onto Si(100) wafers (10–20 Ω cm) with/without a thin film (about 0.3 μm) of SiO_2 at room temperature. The WSi_2 films are deposited by magnetron sputtering cast targets in a sputter deposition system with a constant vacuum of 2×10^{-2} Torr and d.c. power of 0.26 kW [27]. To produce targets for magnetron sputtering, the WSi_2

Disilicide	**Electrical resistivity (μΩ cm)**	
	Target	**Film**
$TiSi_2$	16.9	13–17
$ZrSi_2$	75.8	40–43
$HfSi_2$	62.0	150–260
VSi_2	66.5	67–80
$NbSi_2$	50.4	55–63
$TaSi_2$	46.1	60
$MoSi_2$	21.6	67–80
WSi_2	80.1	50–70
$CoSi_2$	16.0	30.0

Table 4. Specific resistivity of thin disilicide films of refractory metals.

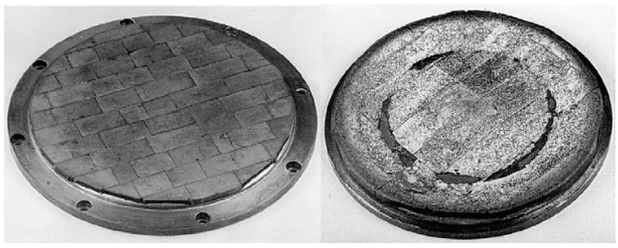

Figure 18. Composite WSi_2 targets for magnetron sputtering: left, new; right, after 150 cycles.

cast blocks of 20×15×5 mm^3 are machined and soldered ultrasonically to copper bases of 152 mm diameter (**Figure 18**). Considering that our purpose is to replace a standard Al metallization with WSi_2 as well as to form the next metallization level, it is not our aim to study a resistivity of contacts of WSi_2 to the *p*-type conductivity layers. Thus, the simplified technological method is used. Following sputtering, the wafers are cleaned in a dilute HF solution for 4 min and rinsed in deionized water before loading into the deposition chamber. The wafers are treated in a buffer etchant for 10 s. A poly-Si layer 0.11 μm thick is deposited onto two wafers. The 0.25 μm thick WSi_2 layer together with a satellite is deposited, and the Al commutation is formed. The WSi_2 layer is reactively ion etched. For removal of the photoresist, a plasma-chemical treatment is employed with additional chemical treatment. Then the wafers are covered with a 0.7 μm borophospho-silicate-glass (BPSG) layer and annealed in N_2 gas. The annealing chamber is purged with N_2 for 10 min before each anneal, and the annealed wafers are allowed to cool in N_2 before removing from the chamber. The BPSG layer is etched off with different chemical procedures.

Various chemical treatments of etching are used on different parts of wafers. Treatment #1 consisted of stripping of the BPSG layer in a buffer etchant for 2 min. In treatment #2, the BPSG layer is stripped off in a similar buffer etchant; however, the layer is etched for 4 min. Treatment #3 involves reactive ion etching of contacts. Treatment #4 includes all three treatments listed above. The input power to sputter composite mosaic targets is as much as 260 W for 30 min for each cycle. Before sputtering, Si wafers are heated to 250–300°C. It has been found that such a procedure is sufficient to produce a clean Si surface. The deposition rate is proportional to the sputtering power at a constant pressure in the sputtering chamber. The sputtering rate and the layer thickness are monitored during deposition with the microprocessor and profilometer, respectively. The deposited silicide films are annealed in vacuum. Some samples are annealed at 950°C in N_2 for 30 min. The film thickness is found to be 200–250 nm. The specific resistivity of cast specimens and of conducting WSi_2 paths as well as contacts to poly-Si layers is measured by the four-point probe sheet resistance method. X-ray phase analysis of cast samples is performed on a Siemens D-500 diffractometer ($\psi = 25°$, Fe-07), and a JXA-5 apparatus is used for local X-ray spectral analysis. Chemical reactions between the film and wafer as well as the distribution of elements are studied by Auger electron spectroscopy together with ion sputtering with a JAMP-10S Auger electron spectrometer. The energy of the primary ion beam is 10 keV, and the current was 5×10^{-6} A. The spot is increased up to 100 μm diameter to prevent a decomposition of the material studied and to lower an electron current density. 1 keV Ar ions are used for sputtering. Instability of an ion gun is no more than 10%. The ion beam diameter is 10 mm. A scanning electron microscope study is performed with a JSM-35S and a Stereoscan 240. Both the elemental composition and elemental depth distribution of 100 nm thick WSi_2 films are analyzed by means of Rutherford backscattering of 1.5 MeV He ions. After annealing of thin refractory metal films deposited in vacuum by magnetron co-sputtering of cast high-purity refractory metals on Si or Si-on-sapphire substrates at 650–700°C, stoichiometric thin disilicide films are produced, which are confirmed by Auger electron spectrometry.

The specific resistivity of cast WSi_2 targets is 50 μΩ cm. It is lower than that of PM targets (70 μΩ cm). Local X-ray spectral analyses of cast targets show that samples are homogeneous. An analysis of the phase composition of laser-deposited films obtained by evaporation (ablation) of cast WSi_2 targets on (100) and (111) Si substrates shows that amorphous WSi_2 forms at substrate temperatures up to 400°C. Above this temperature

it crystallizes and exhibits a mixture of the tetragonal phase and a small amount of the semiconducting hexagonal phase. As the substrate temperature is increased, the amount of the hexagonal phase decreases. At 700°C the film is single-phase tetragonal having a metallic type of conduction. At 750°C, a small amount of a second phase (W_5Si_3) reappears. The experimental results show that, as the pulse frequency is lowered, WSi_2 films become multiphase. In this case the main tetragonal phase of WSi_2 is observed together with a small amount of the hexagonal phase and W_5Si_3. The occurrence of a phase deficient in Si with respect to the disilicide composition might be attributed to the evaporation of the latter. The phase compositions of films obtained after annealing and those deposited immediately onto a hot substrate are similar. Interplanar distances for lines on diffraction patterns of sintered and cast WSi_2 targets and of WSi_2 films deposited from cast targets at 700°C are given in **Table 5**. Phase compositions of films are seen to correspond to those of targets. A small deviation of intensities of measured lines from tabulated ones indicates the presence of texture in samples. Rutherford backscattering data indicate that 100 nm WSi_2 films (the Si/W ratio being approximately 2) are obtained on Si substrates (**Figure 19**). An analysis of the elemental depth distribution shows that this ratio remains constant throughout the film depth. No transitional layer between the film and the substrate (Si or neutral) is observed.

In every case, the tetragonal WSi_2, which coexisted with a small amount of W_5Si_3, is the dominant phase. The microstructural studies of the films deposited on Si(111) at 700°C in a vacuum show that they are homogeneous without ruptures. Being rather thin (30 nm), the films probably copy a substrate surface relief. The SEM studies of the cross sections of the films show

hkl	*d*				
	File data	**PM powder target**	**Cast target**	**Film (laser)**	**Film (magnetron)**
002	3.908	3.911	3.907	3.928	3.927
101	2.970	2.970	2.970	2.962	2.970
110	2.270	2.270	2.268	2.263	2.269
103	2.020	2.025	2.026	2.025	2.025
004	1.961	1.963	1.964	1.965	–
112	1.961	1.963	1.964	1.965	1.964
200	1.603	1.606	1.606	1.601	1.608
114	1.485	1.485	1.484	1.483	1.484
105	1.412	1.412	1.413	–	1.410
211	1.407	1/407	1.407	1.409	–
006	1.304	1.305	1.304	1.308	–
213	1.258	1.258	1.258	1.255	1.257
204	1.241	1.241	1.240	–	–

Table 5. Interplanar distances d_{hkl} of WSi_2 for PM target, cast target, and thin film deposited on Si(100) substrate by laser ablation and magnetron sputtering of cast target.

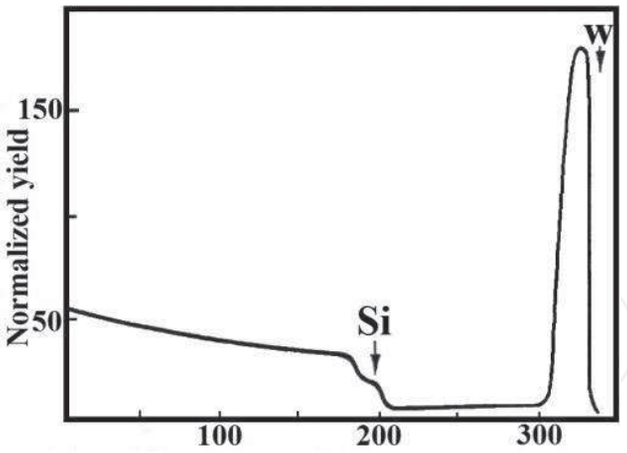

Figure 19. Rutherford backscattering spectra (E_0=1.5 MeV) for film structure WSi_2/Si. Arrows indicate energy positions corresponding to occurrence of W and Si atoms on the surface.

that a boundary between WSi_2 film of 100 nm thick and Si substrate is rather distinct. Similar experimental results are obtained when WSi_2 films are deposited by magnetron sputtering of cast composite targets. Auger electron spectrometry studies of WSi_2 films have revealed a sharp decrease in O and C contents during ion etching of specimens and deepening an analyzing zone. The behavior of O and C at WSi_2 layer is similar. W and Si are homogeneously distributed in the film, which is probably a consequence of interdiffusion. Near SiO_2/WSi_2 interface, there is a rather narrow layer where O is sharply increased and W is sharply decreased; however, Si content after a short decrease remains at a former level. C content remains at the same level as in WSi_2 layer and at the interface. This can be related to the limited solubility of C and C diffusion coefficient in initial WSi_2 film, transition layer, and SiO_2 sublayer. There are no visible changes of these layers after chemical etching as well as no changes of them after etching off the BPSG layers. However, after chemical etching and reactive ion etching, there is a light erosion of the WSi_2 surface. It is found that about 15% of the layer is etched off and the etched surface has a light roughness. The BPSG layer under the WSi_2 layer is partially melted during annealing at 1000°C, so the WSi_2 conducting paths are slightly uneven (curved); however, there are no fractures or cracks. The samples annealed at 900°C have no changes at all. The most visible changes in contacts to the poly-Si and wafers of the samples annealed at 900°C show the appearance of clear distortions in contact sites of wafers without the poly-Si sublayers. The wafers with poly-Si sublayers have no changes. This effect is greater on the samples annealed at 1000°C.

The mean electrical resistance of WSi_2 conducting paths before annealing is 33 kΩ. The mean electric resistivities of WSi_2 conducting paths with poly-Si sublayers are 6.32 and 4.7 Ω/□ after annealing at 900 and 1000°C, respectively. The mean electric resistivities of WSi_2 conducting paths without poly-Si sublayers are 6.65 and 5.6 Ω/□ after annealing at 900 and 1000°C, respectively. Electrical contacts to *p*-type layers are absent, because the layers in the vicinity of contacts can be heavily doped with P from the BPSG layer through the silicide layer or poly-Si. The electrical resistance of contacts to *n*-type conductivity layers on samples without poly-Si sublayers under WSi_2 layers is not reproducible and is very scattered with values up to 20 μΩ cm for 50 contacts. The samples with poly-Si sublayers exhibit

much less scatter in a specific resistance. Thus, $R_{Al\text{-}n+}$ = 360–400 kΩ for 50 contacts on a sample annealed at 900°C; however, the resistance for 50 contacts on a sample annealed at 1000°C is 1.4–1.8 kΩ. $R_{Al\text{-}polySi}$ = 600–700 kΩ for 100 contacts on samples annealed at 900°C; however, the analogous value for 100 contacts on samples annealed at 1000°C is 3.3–3.5 kΩ. All n^+-p-junctions on the large perimeter area of about 16,000 μm^2 and 2120 contacts have leakage currents lower than 0.04 nA at a bias voltage of 15 V. With an increase of the bias voltage, leakage currents increase monotonically up to 0.1 nA at 20 V; however, at 21–22 V junctions have breakdowns.

Analysis of experimental results suggests that WSi_2 deposited during laser evaporation do not form due to Si diffusion from the substrate. This view is supported by experiments on a film deposition on neutral substrates (MgO, Al_2O_3, ZrO_2) where the dominant phase is WSi_2. An important advantage of laser evaporation and magnetron sputtering for depositing films, compared to the annealing technology, is that single-phase films are deposited at a substrate temperature of 700°C, which is 300°C lower than in the case of annealing. Noteworthy is the fact that the tetragonal phase of WSi_2 is obtained at a substrate temperature of 600°C, which is in disagreement with data, which state that this phase nucleates and grows at temperatures above 620°C. The results on room-temperature deposition of thin (30 nm) films on Si substrates (and subsequently annealing at 750°C for 1 min) are also of interest. Their phase composition is analogous to that of films deposited directly on hot substrates. This is very promising technologically. Data on Rutherford backscattering and layer-by-layer X-ray phase analysis suggest that no transition layer exists between the film and the substrate. This is also an advantage compared to the annealing technology. Tetragonal disilicide films deposited by laser evaporation have the resistivity of 50–70 μΩ cm, which conform to values for films deposited by annealing, but it is much lower than for films deposited by magnetron sputtering of PM targets (120 μΩ cm). W and Si are homogeneously distributed across the film, which is probably a consequence of their interdiffusion. Near WSi_2/SiO_2 interface, there is a rather narrow transitional layer, where O and W replace each other. In SiO_2 layer, following the interface, mainly Si and O are found, with low amounts of W and C. Both of these elements are distributed homogeneously in SiO_2 layer by diffusion. O content in WSi_2 layer is a consequence of the fast O diffusion, compared with a self-diffusion of other components of the system, and the high O solubility in W as well as in its silicides.

2.7. Depositing titanium films

Of particular interest are thin films of $TiSi_2$ which due to their low electrical resistivity are the most promising for the inter-element wiring and silicidation areas of the emitters, collectors, and injectors of the bipolar IC, as well the sources, drains, and gates in VLSI. In this connection it is necessary to determine the conditions of formation of $TiSi_2$ films on substrates of single- and polycrystalline Si varying degrees of doping. Here, studies are done of thin films of the $TiSi_2$ formed by a solid-phase reaction of Ti films with the mono- and polycrystalline Si substrate. Thin films of $TiSi_2$ are obtained by magnetron sputtering targets of highly pure Ti, produced by multiple EB vacuum-melting Ti rods and followed by a heat treatment of

the film obtained under nitrogen with O content of 10^{-4}%. The heat treatment is conducted in a diffusion furnace. To reduce the amount of O in the as-deposited Ti films, an annealing is used together with getters. Getters are Si wafers; the front and rear sides of which are coated with Ti films of a thickness 0.1 μm. Plates are positioned before and after experimental samples relative to Ar flow. As substrates, single-crystalline wafers of *n*-Si(100) of 100 mm in diameter, doped with P to the resistance of 4.5 Ω cm, are used. In the case of Ti silicides on the polycrystalline Si, Ti films are deposited on the oxidized beforehand poly-Si of 0.45 μm thick obtained by a silane ammonolysis under a reduced pressure. The thickness of Ti films is measured by the interference method with accuracy of 0.005 μm. A silicide film thickness is calculated from known ratios, knowing the thickness of the metal film, and is measured in a scanning electron microscope of the vertical cleavage of $TiSi_2$/Si structure. The Si substrate temperature during depositing Ti films does not exceed 423°C. Plates are subjected to the standard chemical treatment, and immediately prior to Ti deposition, Si surface is purified by plasma etching. To investigate the degree of influence of both the alloying and impurity-type doping, Si substrates (or a poly-Si film) are subjected to ion doping with B or P at ion energies of 40 and 60 keV, respectively. An annealing Ti film to form $TiSi_2$ is carried out in a diffusion furnace in two steps: at 898K in a nitrogen atmosphere for 30 min and, then, after removing the TiN layer, at 1123K and 30–60 min in a vacuum or Ar atmosphere. A need to anneal in nitrogen causes by the fact that the resulting surface layer consisting essentially of TiN prevented the lateral Ti diffusion which in the real VLSI structures can cause short circuits. The crystal structure of the elemental and phase composition of as-deposited films and silicide films are studied by electron diffraction, scanning and electron microscopy, Rutherford backscattering, as well as X-ray methods, in particular by "moving beam," which allows determining the change of the phase composition across the film thickness. A study is performed on the profiles of the element distribution across the film thickness by Rutherford backscattering with an initial energy of 1 MeV He ions. The scattering angle is 170°. The energy resolution of the detector system is 17 keV. To improve the depth resolution, a sliding experimental geometry is used, in which angles of incidence and scattered ions have a value of 60°. This improvement allows reaching a resolution of 10 nm for Ti and 15 nm for Si, while at normal resolution geometry, they are 20 and 30 nm, respectively. **Figure 20** shows energy spectra of Rutherford backscattering for as-deposited and annealed at 898 K samples. It can be seen (**Figure 20**, spectrum 1) that in the original Ti film, some O is present, as evidenced by the spectrum peak in 350–368 keV energy. The profiles of an element distribution, calculated from the spectrum, allow the thickness of the film to be determined, which is found to be ~3×10^{17} at./cm^2 for the sample. Provided that the volume Ti content is 5.68×10^{22} at./cm^3 and $d = x$ (at./cm^2)/N^* (at./cm^3), Ti film thickness is found to be ~53 μm. O mainly localized in the surface layer of the film of a thickness 1×10^{17} at./cm^2 (15–20 nm), and its concentration does not exceed 25%. An annealing under nitrogen at 898 K and 30 min leads to a redistribution of elements in the surface layer (**Figure 20**, spectrum 2). A layer near the surface is enriched with N atoms and with a small amount of O. At a range of depths $(3.5–5.5)\times10^{17}$ at./cm^2 (a conversion to the unit of length in this case is not correct due to a lack of accurate data on the volume concentration of atoms in the silicide film), the relative concentration of elements corresponds to $TiSi_2$ phase. After chemical or plasma-chemical removal of the fluorine-containing plasma, the surface layer of the film has a phase composition of the $TiSi_2$ with some excess of Si. In

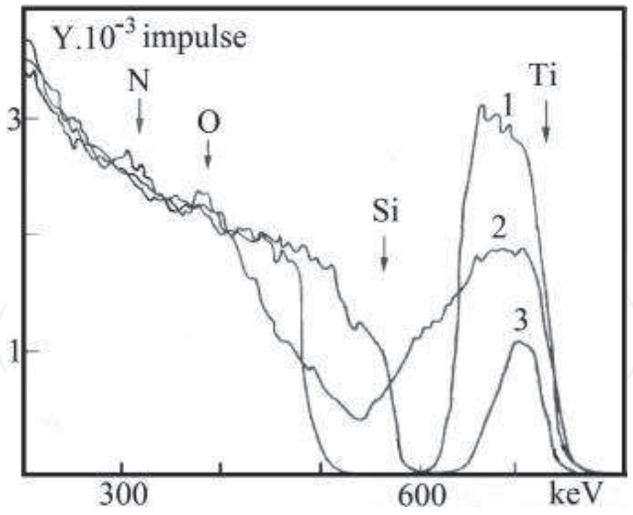

Figure 20. Energy-loss RBS spectra for as-deposited and annealed at 898 K samples. Ti (1) and $TiSi_2$ (2, 3), 2, 3—898K; 2—15 min; 3—15 min after etching off upper layer.

this case, the films do not contain N and O in amounts sufficient for detection by RBS. As a result of X-ray studies, it is established that the formed $TiSi_2$ phase has an orthorhombic C54 structure with lattice constants a = 0.825 nm, b = 0.4783 nm, and c = 0.854 nm, wherein Ti_5O_9 phase is detected on the surface of the film (α = 0.5, 1 deg). The phase composition of films is enough uniform in thickness.

There is no significant difference for $TiSi_2$ films formed on n- and p-type substrates. After the plasma-chemical removal of the surface layer, $TiSi_2$ film is amorphous, and after re-annealing at 1123K, is polycrystalline with an average grain size 0.1–0.3 μm. After the removal of $TiSi_2$ film, precipitates are found on the substrate surface which can be easily removed mechanically. An analysis of these precipitates by electron diffraction has revealed that it is TiN, resulting in the surface film due to its annealing in a nitrogen environment. These results are consistent with RBS (**Figure 20**, spectrum 2). Studies, as well as microreliefs of the substrate surface after the removal $TiSi_2$ film, lead to the conclusion about a fairly clear boundary between $TiSi_2$ film and Si substrate. It can be explained by the mechanism of an interaction of Ti with Si, at which a diffusing dopant is predominantly Si. A second stage of annealing the film at 1023K during 30 and 60 min, after the removal of TiN surface layer, leads to a stabilization of C54 $TiSi_2$ phase. Under these conditions, $TiSi_2$ films have a homogeneous phase composition across their thickness and did not contain the phase of Ti_5O_9. Seemingly it had been removed together with the surface layer. The resistivity of the films of C54 $TiSi_2$ is 13–15 μΩ cm, which is in agreement with known data. With increasing of the substrate doping with P or B, any changes in the phase composition of films are not established: only forming the low-impedance phase C54 $TiSi_2$. It is shown that the low-impedance phase C54 is formed at 963 K during 10–30 min, and its formation is dependent on O content in as-deposited Ti films. Reducing the temperature of the formation of the phase C54 in $TiSi_2$ to 898 K, in this case, may be linked with a sufficiently low O content in as-deposited Ti films. This in turn is determined by the method of producing Ti targets and characteristics of the heat treatment of films associated with additional getters.

2.8. Studying $TiSi_2$/Si interfaces

2.8.1. Short background

A study on the interaction of Ti atoms with a Si surface as chemical reactions at the interface between thin films of Ti and Si is of great interest. It is known that at Ti-Si interface at above 700°C, only $TiSi_2$ can be formed. It is also proved that on an amorphous Si substrate, the growth rate is proportional to the square root of the annealing time (so-called $t^{0.5}$ rule). On a single-crystalline Si substrate, the growth rate of $TiSi_2$ is much slower, and grown $TiSi_2$ films are uneven in a thickness if Ti-Si interface contaminated with impurities. Annealing Ti films on the single-crystalline Si in oxygen or in a mixture of oxygen + nitrogen at 600°C leads to a formation of TiO_2 and $TiSi_2$; however, a heating in N_2 leads to the formation of TiN, Ti_5Si_3, and TiSi without $TiSi_2$. Whereas if to anneal a mixture of Ti_5Si_3 and TiSi at >800°C, it transforms to $TiSi_2$. It is also interesting that at room temperature, Ti and Si do not interact at Ti-Si(100) interface. From electron spectroscopy, similar data for Ti-Si(111) system are also known. However, by RBS experiments a diffuseness of Ti-Si(111) interface at room temperature has been discussed. The main reason of this obstacle for solving the problem is a lack of suitable instruments to identify the reaction products in a Ti-Si system. These instruments should be similar in their capabilities, especially in the depth of the layer to be analyzed. They should be based on a study of Si($L_{2,3}$VV) Auger line shape of, e.g., PtSi system. Thus, it seems that the most distinguished technique which can help us in eliminating the problem is an electron energy-loss spectroscopy (EELS) which is known by its high sensitivity to electronic restructuring of solid surfaces and by possibilities to vary a depth of the layer under analysis [28]. The goal of this study is to obtain electron energy-loss spectra of $TiSi_2$, Ti, and Si and to estimate analytic possibilities of EELS in a study of chemical transformations at Ti-Si interface.

2.8.2. $TiSi_2$/Si interfaces

Single-crystal Si(100) wafers doped with P and Ti rods after EB floating zone melting are used to prepare $TiSi_2$ films by a standard self-aligned silicide method in Ti-Si(100) system. Si wafers with the electrical resistance of 1 Ω cm are previously chemically cleaned from organic impurities and then immersed in HF, followed by washing in a deionized water to remove a natural surface SiO_2. A Si substrate temperature during Ti deposition is about 180°C. The thickness of Ti films is 40–80 nm. $TiSi_2$ films are deposited by magnetron sputtering of Ti targets. A subsequent silicide formation is done by the two-stage high-temperature annealing. The first annealing is carried out at 600–700°C under a N_2 atmosphere for 35–40 min. An excess unreacted Ti, TiO_2, and TiN are removed using an etchant selective to silicide. Silicidation and homogenization are completed at a second annealing at 800°C under Ar atmosphere. The thickness of $TiSi_2$ layers is about 100 nm. The sheet resistance of the films is measured by a four-point probe. The typical resistivity of the Ti layers is 50 μΩ cm; the resistivity of the $TiSi_2$ layers is 13 μΩ cm. An analysis of trace impurities is performed by high sensitive physical methods, such as fast neutron activation, deuteron activation, He^3 ion activation, mass spectrometry with inductively coupled plasma, etc. When registering electron spectra in the analog mode, the relative energy resolution is 0.6%; in a retarding mode, the absolute resolution

does not depend on the energy and is of 0.7 eV. Electron spectra are measured in a spectrometer with a double-pass cylindrical mirror analyzer. To get Auger electron spectra, a monoenergetic (half width, 0.5 eV) electron beam is used with an energy of E_p = 3 keV. For electron energy-loss spectra (EELS), electron beams with energies 100, 400, and 2000 eV are used. The removal of surface contaminations and analysis of the depth distribution of elements are conducted in combination with sputtering of the sample surface by 2 keV Ar ions with 9 μA cm^2. A residual gas pressure in the test chamber of the spectrometer is 5×10^{-8} Pa, and Ar pressure during sputtering was 3×10^{-3} Pa. An elemental analysis is performed by Auger spectroscopy using factors of an elemental sensitivity.

The electrical properties of metal and silicide layers in Ti-Si system depend strongly on impurities. Thus, it is very important to use Ti targets with the highest purity for the sputter. This means a low content of gas-forming interstitials and metal impurities. After a complex of vacuum procedures, Ti designed for magnetron sputtering contains trace impurities according with **Table 1**. In **Figure 21** a distribution of elements in $TiSi_2$ films is shown. A subsurface area, after sputter over 9 min, contains, besides $TiSi_2$, certain amounts of TiN and SiO_2. These data can be drawn from an analysis of the form Si ($L_{2.3}VV$) lines and an intensity ratio of Ti (LMV) (418 eV) to Ti (LMM) (387 eV). A composition of the interior of films, sputtered for 30 min (from 10th min etching up to the 40th min), is close to $TiSi_2$. A total content of gas-forming interstitials (C, O) in this area of films is not greater than 1–2 at.%. Note that the ratio of peak intensities of Ti (418 eV)/Ti (387 eV) lines in $TiSi_2$, measured at a modulation voltage of 3 V, is equal to 1.13. This value is very close to 1.2. For metal Ti this value is 1.6; thus, an intensity ratio of Ti (418 eV)/Ti(387 eV) may be used for analytical purposes when estimating a number of Ti atoms in reaction with Si. Si($L_{2.3}VV$) Auger line shape in the transition region from $TiSi_2$ to Si varies insignificantly at layer-to-layer sputtering. Such behavior is known as a characteristic of refractory metals silicides [29, 30]. It is noted that in the range of kinetic energies from 75 to 85 eV, however, variations of electron spectra nevertheless happened. It seems that this fact is difficult to use for analytical purposes because of a low relative intensity of this spectral region. Thus, a shift of Si ($L_{2.3}VV$) line by 1.3 eV, observed in the initial stage of the formation of $TiSi_2$, seems to be due to the fact that relaxation conditions during the Auger process in

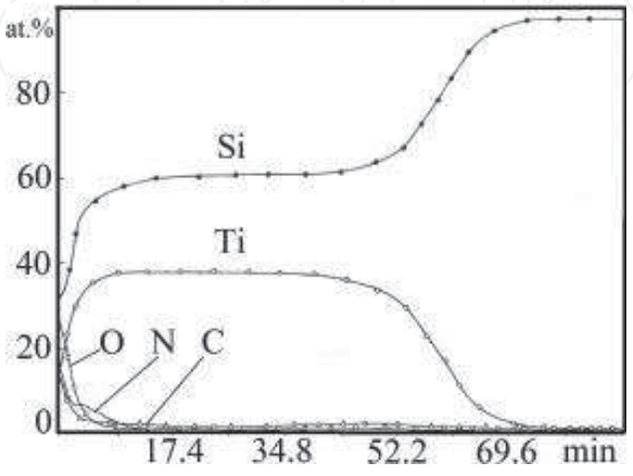

Figure 21. Profile element distribution in $TiSi_2$/Si(100) structure, obtained by AES during etching with argon ions.

the thin Si layer on the surface of Ti or $TiSi_x$ films differ from those in a bulk Si. The changes observed in the low-energy part of the Auger spectrum are due to changes in Auger energy-losses spectra. Therefore, EEL spectra are studied using a monochromatic electron beam as an excitation source. EEL spectra, which are obtained in reflection geometry, provided data on excitations in layers of 0.3–2 nm thick. Thus, a contribution of surface excitations, as a rule, is of a great importance for these spectra. The value of this contribution depends on both the mean-free path of electrons in analysis and the experimental geometry. In addition to a quantitative interpretation of reflection, EEL spectra should be taken into account not only multiple small-angle electron scattering but large-angle scattering as well.

For analytical purposes, some of the parameters of the measured spectra are often possible to use without further mathematical processing. For example, energy positions of major peaks in EEL spectra are slightly depended on a shape of multiple scattering histories. It is of interest to compare measured energy locations of intense peaks in EEL spectra of $TiSi_2$ at various energies of primary electron energies of bulk and surface plasmons, estimated in a free-electron approximation: $\omega_p = (4\pi ne^2/m)^{1/2}$, where n a density of valence electrons per volume unit, $\omega_s = \omega_p/\sqrt{2}$ (see **Table 6**). An estimation of the valence electron density is carried out using known values of specific densities $\varrho_{Ti} = 4.51$ g/cm^3 and $\varrho_{si} = 2.33$ g/cm^3. For $TiSi_2$ a density of 4.043 g/cm^3 measured by X-ray analysis is used [25]. It should be emphasized that tabulated energy values differ from maxima locations in EEL spectra recorded in a form of the second derivative $d^2N(E)/dE^2$ for $E_p = 153$ eV [31]. A comparison of energy shows that a location of the main peak in EEL spectrum with $E_p = 100$ eV of $TiSi_2$ is very close to the surface plasmon energy $\hbar\omega_s = 13.9$ eV and with $E_p = 2$ keV, which is close to the bulk plasmon energy. The contributions of both the bulk and surface plasmons in EEL spectrum at $E_p = 400$ eV are comparable in a magnitude. As the energy of primary electrons increases, spectral peaks become narrower. A total width at a half height of the mean peak, $\Delta_{1/2}$, received by this method, is decreased from 19 eV at $E_p = 100$ eV to 10 eV at $E_p = 2$ keV. This parameter is influenced by the background of electron inelastic scattering. Thus, a peak width at 3/4 height, $\Delta_{3/4}$, seems more analytical. A comparison of EEL spectra of Ti and Si with the spectrum of $TiSi_2$ for different energies of primary electrons is done. The spectra differences can be observed for all E_p, but the most analytic spectra are spectra with narrow peaks.

Considering spectra at $E_p = 100$ eV, when a mean-free electron path is minimal—0.4 nm, the locations of the main maxima in the spectra are different, but due to a complicated shape of spectra, the energy locations cannot be the main analytical functions. It seems that more characteristics are widths $\Delta_{3/4}$ that are equal to 16.3, 13.7, and 10.5 eV for spectra of Ti, $TiSi_2$,

Sample	M			$\hbar\omega_s$	
	100	**400**	**2000**	**Ref. [31]**	$(4\pi ne^2/m)^{1/2}$
Si	15.2	16.8	17.0	16.8	16.6
Ti	8.4	14.6	17.4	19.2	17.7
$TiSi_2$	13.2	18.0	19.0	17.2	19.8

Table 6. The maximum positions M of the EEL spectra and plasmon energies $\hbar\omega_p$ (in eV).

and Si, respectively, at E_p=100 eV. By measuring values for thin Ti-Si films, their presence can be found in the layer of 0.4 nm thick. Of course, there is a problem of distinguishing a simple mixture of Ti+Si and $TiSi_2$ with EEL spectra. The artificial spectrum of a simple unreacted Ti+Si mixture is produced by a superposition of EEL spectra normalized to the elastic peak intensity and taken with corresponding weights. It can be shown that at low primary electron energy (E_p=100 eV), when a peak width is greater, a value of $\Delta_{3/4}$ close to that for $TiSi_2$ may be received at a certain mixture composition. In this case, the simple unreacted Ti+Si mixture and a composition of $TiSi_2$ layer after a chemical reaction may be distinguished, because (*a*) the location of the maximum in the spectrum of the mixture is close either to the location of the maximum in Ti spectrum (8.4 eV) or Si spectrum (15.2 eV), excluding a small transition region of compositions near Ti-Si=1; (*b*) with coincident maxima in spectra, the *a* location on the energy-loss scale corresponds to 29.9 eV for $TiSi_2$ and 24.6 eV for the mixture of Ti+Si spectrum. With E_p = 2 keV, it is not difficult to distinguish EEL spectrum of $TiSi_2$ from those of the mechanical Ti+Si mixture, because for mixture spectra the location of the main maximum are within 17–17.4 eV, whereas for $TiSi_2$ this value is 18.8 eV (**Figure 22**). Besides, the EEL spectrum of $TiSi_2$ exhibits also a second maximum at energy of ≈38 eV that is missing in spectra of Ti-Si mixture. Thus, EELS enables one to carry out an analysis of an interaction of components in Ti-Si system with a high depth resolution.

2.9. Depositing cobalt disilicide films by laser ablation

2.9.1. Short background

An interest in silicides of refractory metals has increased significantly due to their great potential as a material of low resistance contacts, gates, and interconnects of the thin-film metallization of Si integrated circuits. The principal possibility of obtaining pure $CoSi_2$ targets by vacuum-metallurgical methods is developed [15, 32]. The optimal conditions of sputter targets have been revealed, providing a deposition of $CoSi_2$ films with the specific resistivity of 30 μΩ cm. By X-ray

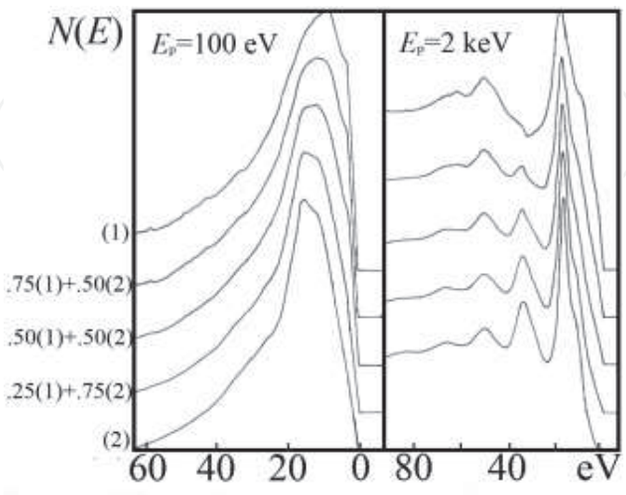

Figure 22. Electron energy-loss spectra of Ti (1) and Si (2); a linear combination of these spectra with different weight fractions.

diffraction patterns in the sliding beam incidence and Rutherford backscattering of He ions, the phase and elemental composition of the films are investigated. Currently in microelectronics two methods are used for producing silicide thin films. The first of them is a deposition of metal films on a Si surface, followed by high-temperature annealing. The second is composed of sputtering targets made of a silicide powder. Unfortunately, the manufacture of targets using PM technologies usually leads to instabilities of sputtering and contamination of targets, which increase the specific resistivity of deposited films. Thus, vacuum-melting procedures, seemingly, become an optimal and logic decision for the production of targets. In recent years, interesting results have been obtained by the method of sputtering metal and semiconductor films by a laser radiation which has several advantages over other methods of depositing films. It is compatible with high vacuum setups and does not require using a working gas. When the laser radiation flux density in the affected area exceeds 10^{-9} W s^{-2}, the evaporation of the target material takes place without a formation of a liquid phase (laser ablation), so that the stoichiometry of the film corresponds to the composition of the target. This is an excellent opportunity of using laser deposition films for substances with a complex stoichiometry. A high efficient sputter rate (10^{-6} A s^{-1}) supports reducing the contamination of the film by the residual gasses of the vacuum system. Due to the high energy of condensed atoms (10^5 K), it is possible to obtain epitaxial films at lower substrate temperatures than for other methods. Here, experimental results of our studies are presented of obtaining the $CoSi_2$ films by laser ablation of cast high-purity targets.

2.9.2. Depositing cobalt disilicide films

As the initial materials for preparing $CoSi_2$ targets are used a polycrystalline Si of 99.999% purity and a commercial Co. To further increase the purity of Co, a double EB vacuum refining is performed [15]. A typical content of impurities after chemical and EB floating zone purifying is shown in **Table 1**. For the preparation of $CoSi_2$ of a stoichiometric composition, the mixture of high-purity Co and Si is melted in a vacuum induction furnace in high purity Ar. The melt is poured into molds receiving rods of 10 mm in diameter and 150 mm in length. The resulting bars are subjected to double floating EB zone melting. $CoSi_2$ targets are of 20×15×5 mm. They are evaporated by laser in a vacuum setup. A solid-state Nd-glass laser is used with wavelength of 1.06 μm, pulse repetition rate of 10 Hz, and pulse energy of 0.8 J. The vacuum chamber is evacuated to a vacuum of 1×10^{-6} Torr using a turbo pump. The laser beam is focused by a lens; the focal spot size is 2–3 mm. A distance between the target and substrate is 70 mm. For heating the substrate, an infrared heater with halogen lamps is used. The Si(100) wafers, mica, MgO, Al_2O_3, and ZrO_2 are used as substrates. Substrates are subjected to chemical cleaning and then immediately prior to depositing are heated at 850° for 10 min in vacuum. The temperature of substrates is varied in the range of 100–800°; the deposition time is varied from 5 to 20 min. A film thickness is measured using a profilometer and is from 300 to 1500 Å. The specific resistivity of bulk samples and thin films is measured by the four-point probe method. XRD data of $CoSi_2$ samples show that they are a single phase and composed of stoichiometric $CoSi_2$. A local X-ray analysis of cross sections has revealed the homogeneity of the chemical composition of $CoSi_2$ samples. Double EB melting of $CoSi_2$ ingots does not lead to a significant change in its phase composition. The specific resistivity of bulk samples of $CoSi_2$ is 16–20 μΩ cm, which is close to the data, obtained for single

crystals of $CoSi_2$. The samples prepared by the PM technology have an electrical resistivity of 65–68 μΩ cm. An important advantage of the method of depositing films by the laser ablation compared with annealing a Co-Si system is a deposition of films at a substrate temperature of 700–800°C. This temperature is 200–300°C lower than in the case of annealing. In addition, the film does not contain Ar, which usually occurs in magnetron sputtering. The results of XRD of the cast target and films obtained in the range of the substrate temperature from 200 to 750°C show that as-deposited films are textured, and with increasing the substrate temperature, the degree of texturing increases (when the temperature increases, the amount of equiaxed polycrystalline grains decreases sharply). At the substrate temperature of 400°C, films are disilicides $CoSi_2$ (**Table 7**). The films deposited at other substrate temperatures are bi-phasic, and at 200°C together with the $CoSi_2$, which is the main phase, an excess of Si is presented as well. At temperatures of 600, 700, and 750°C together with the main phase ($CoSi_2$), a small amount of CoSi is found. Sputtering onto substrates ZrO or MgO at 700°C also affords films consisting of $CoSi_2$ and a small amount of CoSi. From RBS, at the films deposited at the substrate temperature of 600°C, the ratio of Si/Co is about 2 (**Figure 23**). The

hkl	$CoSi_2$		Target		Film	
	d_{tab}	*I*	*d*	*I*	*d*	*I*
111	3.096	90	3.099	80	3.118	82
220	1.898	100	1.897	100	1.897	82
311	1.618	23	1.616	24	1.620	14
222	1.548	1	–	–	–	–
400	1.340	17	1.340	12	1.346	13
311	1.230	11	1.230	10	1.231	18
422	1.095	2	1.094	20	1.094	22

Table 7. Interplanar distances of $CoSi_2$ for the cast target and the film deposited on the Si(100) substrate at 400°C.

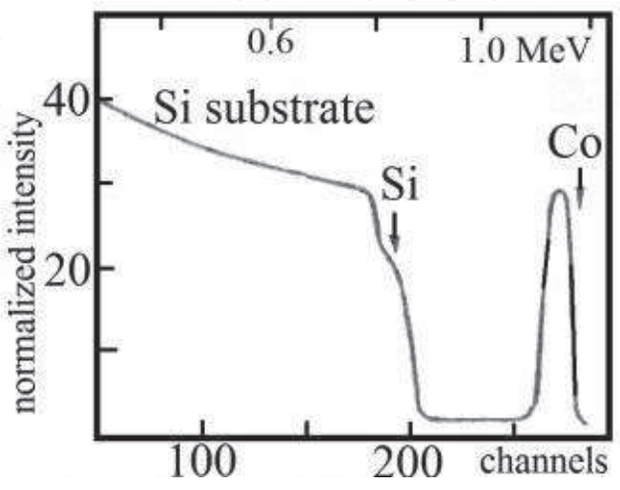

Figure 23. RBS spectra of the $CoSi_2$ film structure. Arrows indicate the position of energy corresponding to surface bedding Co and Si atoms.

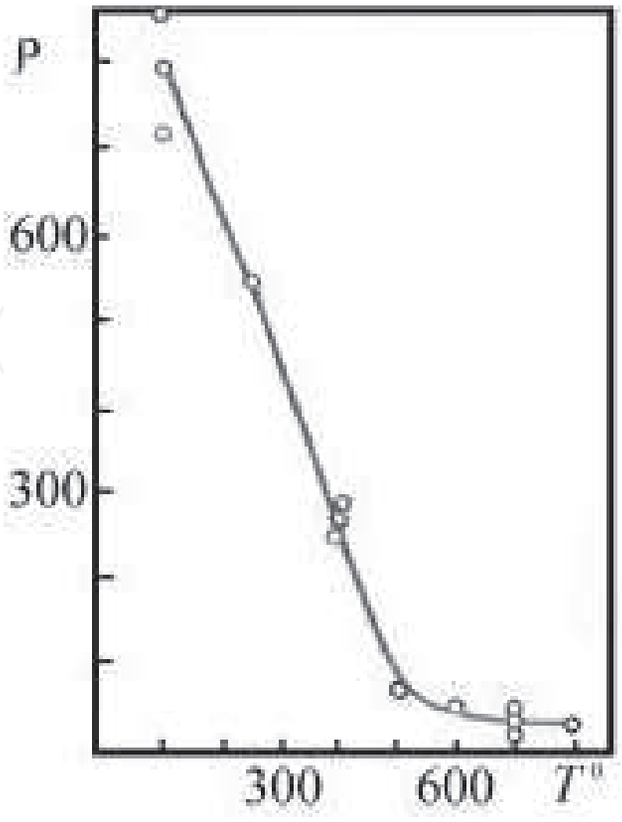

Figure 24. The dependence of the specific resistivity of $CoSi_2$ films on Si(111) on substrate temperature.

thickness of the stoichiometric film is about 600 Å. The transition layer between the film and the substrate is not detected. **Figure 24** shows the dependence on the substrate temperature of the specific resistance of $CoSi_2$ films of 600 Å thick on Si(100). It is seen that with increasing the substrate temperature, the specific resistivity of the film decreases. Especially sharply it is at the range of 100–500°C where the specific resistivity is reduced by about one order of magnitude (from 800 to 60 μΩ cm). In the range of 600–800°C, the specific resistivity depends weakly on the temperature and reaches the level of 30 μΩ cm. The relatively high specific resistivity values of $CoSi_2$ films at low temperatures can be attributed to the presence of the excess Si in the composition of films. At high temperatures, the predominance of the substrate composed of $CoSi_2$ films, as well as increasing the degree of texture of samples, leads to a sharp decrease in their resistivity, which explains the behavior of the curve depending on the specific resistivity.

3. Key findings

1. The multiple EB floating zone melting, multiple EB melting, vacuum levitation melting, and electric arc vacuum melting have been successfully used together with chemical techniques of a preliminary purifying by halides and ion exchange of refractory metals. Preparing highly pure refractory metals containing trace contents (on the level of ppm and ppb) of gas-forming interstitials as well as radioactive impurities and light metals

is demonstrated to be possible. To extend a range of the analyzing limitations, the advanced analytic techniques are used, which allowed to determine the real trace contents even on the lowest level—of ppb. It is also shown that both the production methods of cast targets and sputter conditions have a strong effect on the physical properties of deposited refractory metal thin films. By indicating ways to evaluate interstitials and other impurities in as-deposited films, this approach allows one to determine regimes of sputtering providing the deposition of high-purity metallic layers with the optimal specific resistivity.

2. Impurity contents in thin TiW films deposited by co-sputtering of cast metal targets are quite low comparing with impurity contents of films deposited by magnetron sputtering of PM targets under similar conditions. The specific resistivity of TiW thin films strongly depends on Ti/W ratio. The resistivity of thin films of pure W and Ti is close to tabulated ones for bulk metals. The resistivity of films increases gradually as the Ti/W ratio changes from those for the pure W to the pure Ti; however, it is worth to mention that the resistivity of quasi-alloy films is always higher than those of pure metals.

3. TiW films, deposited by magnetron sputtering of highly pure composite cast Ti/W targets, are grown and studied by AES, XRA, and XRD. AES data showed that Ti/W ratio in TiW films is nearly constant during the sputtering lifetime of composite targets. X-ray spectral analysis of contacts with TiW barrier layers, obtained at the increased sputtering power, is partly due to the higher dispersion of the microstructure. XRD data show that TiW films are solid solutions of Ti in W matrix with increased W lattice parameters. The structure is found to be a solid solution of α-Ti in *bcc* α-W with a lattice parameter of 0.318–0.323 nm. It is also shown that a relative increase in W lattice parameters depends on physical conditions of Si substrates or sublayers on which films are deposited.

4. Schottky diodes with TiW films exhibit a higher level of current leakage than diodes with Mo films, although in both cases, leakage currents are not an obstacle for the commercial use of these highly pure refractory metals as Schottky diode barrier layers. The great advantage of Schottky diodes with Si/PtSi/TiW/Al structure is a high thermal stability of the direct breakdown potential.

5. The refractory metal silicides are very brittle. Thus, one of the experimental approaches to produce these silicides would be used to cast refractory metal silicide targets by HF levitation melting and attaching cast silicide pieces to copper bases by ultrasonic soldering. Vacuum melting (and casting) of silicides solves three main problems of the silicide thin-film deposition: easy production of samples of desired geometries, any chemical compositions, and high purity of silicide thin films. For magnetron sputtering, the composite cast WSi_2 and $MoSi_2$ targets of 152 mm in diameter are produced. Our study has revealed perspective possibilities of depositing WSi_2 films by both the laser evaporation of small cast targets and magnetron sputtering of composite cast WSi_2 targets. The conditions and regimes of the laser evaporation and magnetron sputtering of cast targets ensure the formation of single-phase WSi_2 films with the optimal specific resistivity of 50–70 $\mu\Omega$ cm. Films about 200–250 nm thick are shown to be effective diffusion barriers and conducting paths at annealing temperatures up to 900–1000°C. Leakage currents do not deteriorate diode junctions having WSi_2 layers with poly-Si sublayers.

6. The principal possibilities of obtaining high-purity cast targets of $CoSi_2$ and WSi_2 by crystallization from its liquid phase using a set of metallurgical methods are studied. The modes of the laser evaporating (ablation) have revealed to ensure a stable deposition of stoichiometric $CoSi_2$ and WSi_2 films with the specific resistivity of 30 and 50 μΩ cm, respectively. The results of XRD of cast targets and films obtained in the range of the substrate temperature from 200 to 750°C show that the as-deposited films are textured and with increasing substrate temperature, the degree of texturing increases (when the temperature increases, the amount of equiaxed polycrystalline grains decreases sharply). It should be emphasized that at a substrate temperature of 400°C, as-deposited films are stoichiometric disilicides $CoSi_2$ and WSi_2.

Author details

Vadim Glebovsky

Address all correspondence to:glebovs@issp.ac.ru

Institute of Solid State Physics, The Russian Academy of Sciences, Russia

References

[1] Benzing WC. Shrinking VLSI dimensions demand new interconnection materials. Electronics. 1982;**55**(17):116-119

[2] Ortner HM, Wilhartitz P, Grasserbauer M, Virag A, Friedbacher G. Ultrapurity in metallurgy—Facts and fiction. Kontakte (Darmstadt). 1987;**3**:3-7

[3] Ortner HM, Bloedorn W, Friedbacher G, Grasserbauer M, Krivan V, Virag A, Wilhartitz P, Wuensch G. Ultrapurity in metallurgy—With special reference to refractory metals application in microelectronics. Kontakte (Darmstadt). 1988;**3**:38-52

[4] Iwata S, Yamamoto N, Kobayashi N, Tereda T, Mizutani T. A new tungsten gate process for VLSI applications. IEEE Transactions on Electron Devices. 1984;**31**(9):1174-1179

[5] Yamamoto N, Kume H, Iwata S, Yagi K, Kobayashi N, Mori N, Miyazaki H. Fabrication of highly reliable gate MOS VLSI's. Journal of Electrochemical Society. 1986;**133**(2):401-407

[6] Hoffman V. Tungsten-titanium diffusion barrier metallization. Solid State Technology. 1983;**26**(6):119-126

[7] Sawada S. On advanced sputtering targets of refractory metals and their silicides for VLSI application. In: Proc. 12th International Plansee Seminar. Vol. 1; Reutte/Tirol, Austria, Austria. 1989. pp. 201-210

[8] Glebovsky VG. Preparation of high purity refractory metals for thin film metallization. In: Proceedings of International Symposium on Rare Metals. Vol. 1; Kokura, Japan. 1990. pp. 343-353

[9] Fromm E, Gebhardt E. Gase und Kohlenstoff in Metalle. Berlin: Springer Verlag; 1976

[10] Shipilevsky BM, Glebovsky VG. Competition of bulk and surface processes in the kinetics of hydrogen and nitrogen evolution from metals into vacuum. Surface Science. 1989;**216**:509-527

[11] Ishigami T, Ishihara H, Shimotori K. High purity Ti sputter targets for VLSI. Toshiba Review. 1987;**161**:38-41

[12] Klimenko GL, Blohin AA, Glebovsky VG, Ermolov SN, Mayorov DY, Kopiryn AA. Production of high purity W and Mo powders by ion exchange. Russian Metallurgy (Metalli). 2001;**3**:49-55

[13] Stinov ED, Sidorov NS, Glebovsky VG, Karandashev VK. The combined purification of titanium. Russian Metallurgy (Metalli). 2004;**6**:49-53

[14] Sidorov NS, Glebovsky VG, Shtinov ED. Refining of nickel by chemical & solidification methods. Russian Metallurgy (Metalli). 2011;**7**:610-615

[15] Glebovsky VG, Sidorov NS, Stinov ED, and Gnesin BA. Electron-beam floating zone growing of high purity cobalt crystals. Materials Letters. 1998;**36**:308-314

[16] Glebovsky VG. Physical and technological aspects of processing high-purity refractory metals. In: Glebovsky VG, editor. Recrystallization in Materials Processing. Rieka, Croatia: InTech Publishing House; 2015, 211p

[17] Amazawa T, Oikawa H, Shiono N, Honma N. Extended Abstracts of 16th Conference on Solid State Devices and Materials; Kobe, Japan. 1984; p. 269

[18] Yamamoto N. A study on the low resistivity gate electrode interconnections for ultra high density devices [doctoral thesis]. School of Engineering, Tokyo University; Tokyo University 1986

[19] Glebovsky VG, Markaryants EA. Thin film metallization by magnetron sputtering from highly pure molybdenum targets. Journal of Alloys and Compounds. 1993;**190**:157-160

[20] Glebovsky VG, Markaryants EA, Titov EV. Deposition of W-Ti thin films by magnetron sputtering. Materials Letters. 1994;**20**:89-93

[21] Babcock SE, Tu KN. Titanium-tungsten contacts to Si: The effects of alloying on schottky contact and silicide formation. Journal of Applied Physics. 1982;**53**(10):6898-6905

[22] Babcock SE, Tu KN. Titanium-tungsten contacts to Si: II. Its stability against aluminum penetration. Journal of Applied Physics. 1986;**59**:1599-1605

[23] Glebovsky VG, Yastschak VY, Baranov VV, Sackovich EL. Properties of tungsten-titanium thin films obtained by magnetron sputtering of composite targets. Thin Solid Films. 1995;**257**:1-6

[24] Glebovsky VG. Metallurgical aspects of preparation of high purity refractory metals for thin film metallization. In: Proceedings of 12th International Plansee Seminar. Vol. 3; Reutte/Tirol, Austria, Austria. 1989. pp. 379-389

[25] Murarka SP. Silicides for VLSI Applications. Academic Press, New York; 1983

[26] Glebovsky VG, Oganyan RA, Ermolov SN, Stinov ED, Kolosova EV. Preparation of tungsten disilicide thin films by laser evaporation. Thin Solid Films. 1994;**239**:192-195

[27] Glebovsky VG, Ermolov SN, Motuzenko VN, Stinov ED. Thin silicide films deposited from cast silicide targets. Materials Letters. 1998;**37**:44-48

[28] Shulga YM, Glebovsky VG, Dulinets YC, Rubtsov VI, Borodko YG. Electron energy loss spectroscopy as an analytical tool in the study of $TiSi_2$/Si interfaces. Materials Letters. 1993;**15**:325-330

[29] Butz R, Rubloff GW, Tan TY, Ho PS. Chemical and structural aspects of reaction at the Ti/Si interface. Physical Review B. 1984;**30**(15):5421

[30] Raaijmakers IJMM. Fundamental aspects of reactions of titanium-silicon thin films for integrated circuits [PhD thesis]. Philips Research Laboratories, Eindhoven; 1988

[31] Sharma JKN, Chakraborty BR, Shivaprasad SM. Chemical shifts of Si and Ti in $TiSi_2$ studied by AES, SEELS and IXPS. Journal of Vacuum Science & Technology A. 1988;**6**:3120

[32] Glebovsky VG, Oganyan RA, Ermolov SN, Kolosova EV. Deposition of cobalt disilicide thin films by laser ablation. Thin Solid Films. 1994;**248**:145-148

IntechOpen